UCSF
UC San Francisco Electronic Theses and Dissertations

Title
The cell cycle dependent regulation of microtubule dynamics

Permalink
https://escholarship.org/uc/item/59503938

Author
Belmont, Lisa D.

Publication Date
1995

Peer reviewed|Thesis/dissertation

eScholarship.org Powered by the California Digital Library
University of California

ACKNOWLEDGMENTS

When I first started graduate school I found myself with an incoming class filled with bright and supportive people. My classmates continued to be a source of support, both intellectually and emotionally for the next several years. I am extremely indebted to all of my classmates for this, I really don't know if I could have made it through the early years of graduate school without them. When I joined the Mitchison lab, I relied heavily on Linda Wordeman for helpful advice, humor, moral support, and friendship. She really helped me to become a biochemist and always had confidence in my ability to do good science. I will be forever grateful for her support. I also wish to thank Tony Hyman, whose help was essential on the first part of my project, and whose enthusiasm and interest kept me working day and night. I wish to thank all the members of the annex, Linda, Jody, Arshad, Ann, Julie, and Aneil, for helping to make a dark hole a brighter place to work. I especially thank Ann for her beautiful artwork and warm sense of humor.

When we moved into a brighter annex, I was fortunate to have Jody Rosenblatt as my baymate. She provided great conversation, great music, put up with my mood swings, showed an interest in my project, and made the annex a fun place to work. I also want to thank Arshad Desai for generously sharing reagents, protocols, advice, and cheetos. I want to thank Jason for requesting loud and obnoxious music while doing frog preps, for giving me Tris buffer for my last gel, and for giving me buffer the next 20 "last gels". I want to thank Heather for showing an interest in my project and wanting to take it on when I leave.

When I ventured back to the main lab to pH buffers or make tea, Louise, Suzie, and Mimi, Peg, Matt and Claire were always friendly and

welcoming. I especially want to thank Louise and Suzie for enthusiastically encouraging me to travel. Arshad and Claire have been especially helpful in the last few weeks in giving me advice and reagents for the immunodepletion of Op18 from Xenopus extracts.

When I ventured even further out of the lab into other UCSF labs I found many helpful scientists. I want to thank Bill Theurkoff for advice on microtubule biochemistry, Josh Niclas for help with the DIC microscope, Jeremy Minshull and Aaron Straight for advice, protocols and reagents for the frog/yeast project. I wish to thank Christine Field for giving me encouragement on my project and helping to improve the social dynamics of the lab. I also thank all the members of Microtubule Group for comments and suggestions, and all the members of Club Jameson for making Fridays fun.

Being a student in Tim Mitchison's lab has been an interesting journey. When I joined the lab I was new to being a graduate student, and Tim was new to being a PI. We both fumbled around, figuring out what we were supposed to do in these new roles, and we have both changed enormously in the six and half years that I have been in the lab. I want to thank Tim for several things. First and foremost, he is a great role model. By that I mean that not only is Tim a great scientist and creative thinker, but he really enjoys being a scientist. It has been very important during my graduate school years to be able to look at Tim and see that this path can work for some people. Secondly, Tim has filled the lab with great people doing great science. From the time I was rotating until now, every group meeting was about an interesting project in an exciting area of research that I looked forward to each week. Lab members are not only interested, but genuinely supportive and helpful. The third thing I wish to thank Tim for is technical advice on my

project and helping me to overcome my fear of trying new techniques. It is rare for a PI to do things such as go into the cold room with a student to help them do a centrosome prep, or help in the lab tubulin preps. Seeing how Tim approaches bench work with enthusiasm and confidence has inspired me to try many new techniques and hammer away at difficult projects.

I want to thank the other members of my thesis committee, Bruce Alberts, Ron Vale, and Andrew Murray. I want to thank Bruce for saying , so what if isn't sensitive to proteases, just purify it. I want to thank Ron for always showing interest in my project, and being very generous with the use of microscopes in his lab. I wish to thank Andrew for forbidding me to construct a new library for a yeast project that I wanted to start late in graduate school. Without that advice, I would probably still be slaving away on some project instead of writing this.

Finally, I wish to thank Rachel Longan for her love and support during these final years of graduate school, I know it has not always been easy to put up with stress induced mood swings and long hours in the lab. Thanks, all of you, I couldn't have done it alone.

The Cell Cycle Dependent Regulation of Microtubule Dynamics

Lisa D. Belmont

Abstract

Microtubules have much shorter half lives in mitotic cells than in interphase cells, and this difference in microtubule dynamics is thought to be essential for spindle assembly and functional. To further characterize the cell cycle difference in microtubule dynamics, we used rhodamine tubulin to image individual microtubules in interphase and mitotic extracts of *Xenopus laevis* eggs. The primary difference was a 6 fold increase in the catastrophe frequency of mitotic microtubules.

To study the mechanism of regulation of catastrophe frequency, I developed a rapid assay to identify inhibitors of microtubule assembly. Using this assay, I identified two activities that increase the catastrophe frequency of microtubules. One was purified and shown to be identical to a previously identified protein named Op18 or stathmin. This protein binds tubulin dimers and inhibits stabilization of microtubules by taxol.

The other active fraction was shown to result from something that is approximately 2000 Da, as estimated from a sizing column. This activity was never purified to homogeneity and identified. However, studies on its effect on microtubule dynamics suggest that it may increase catastrophe by increasing the off rate of GTP tubulin. This model is further supported by data showing that the active fraction destabilizes microtubules polymerized with a very slowly hydrolyzable GTP analog, GMPCPP, without increasing the rate of hydrolysis of this analog.

Timothy J. Mitchison, Ph.D.

Table of Contents

Introduction.....1

Chapter 1.....12

Table 1 Dynamic paramters of MTs in extracts.....16

Table 2 Mean lengths of MTs in extracts.....17

Table 3 Dynamic parameters at varied tubulin concentration....17

Table 4 Release of MTs from Centrosomes.....19

Fig 1 Preparation of extracts of defined cell cycle state.....14

Fig 2 MTs in interphase and mitotic extracts.....15

Fig 3 MT length vs. time.....16

Fig 4 MTs in a cycling extract.....18

Fig 5 MT motility in extracts.....19

Chapter 2.....24

Table 1 Purification 59

Table 2 Effects on dynamic instability.....60

Fig 1 Rapid rhodamine tubulin assay.....54

Fig 2 Purification gel.....55

Fig 3 Protease sensitivity.....56

Fig 4 Sizing column on active fraction.....57

Fig 5 Binding of Op18 to tubulin dimers.....58

Chapter 3.....61

Table 1 Purification 75

Table 2 Effects on dynamic parameters of MTs.....75

Fig 1 Models for effects on dynamic parameters.....76

Fig 2 MT growth rate and catastrophe frequency.....77

Fig 3 Destabilization of GMPCPP MTs.....78

Fig 4 Hydrolysis of GMPCPP.....79

Discussion.....80

Fig 1 Model for cell cycle regulation of MT dynamics.....87

Appendix 1 MT/MAP depletion of extracts.....88

INTRODUCTION

Much of the structure and organization of a cell is derived from the cytoskeleton. Microtubules (MTs), one of the major components of the cytoskeleton, are long rigid polymers of tubulin. These polymers are nucleated from the microtubule organizing center (MTOC) and provide spatial organization in a cell as well as a network along which organelles are transported. When a cell goes through mitosis, these MT networks are broken down and MTs assemble into a mitotic spindle that segregates chromosomes into the daughter cells. What makes MTs so useful for the cell are not so much their strength and permanence as their capacity for rapid change and reorganization. MTs assemble from tubulin subunits and use the energy of nucleotide hydrolysis to favor subsequent disassembly. It is this capacity for self assembly and disassembly that allow the construction of complex structures such as mitotic spindles. MTs will self assemble from tubulin *in vitro,* and in cellular extracts with other proteins and chromatin, MTs can assemble into bipolar spindles. This ability to assemble into complex highly organized structures by rapidly sampling many configurations makes the study of MTs an excellent model for the evolution of complex structures.

In vitro, MT polymers interconvert between phases of slow growth or rapid shortening, with abrupt transitions between the two phases (Mitchison and Kirschner, 1984). Transitions from growing to shrinking are called catastrophes and transitions from shrinking to growing are called rescues. Growth and shrinkage is due to addition or loss of tubulin subunits from the ends of MTs, respectively. This behavior, termed dynamic instability, has been observed in cellular extracts (Belmont et al., 1990,

Gliksman et al., 1992) and *in vivo* in many cell types (Cassimeris et al., 1988, Shelden and Wadsworth, 1993). Microtubules have an intrinsic polarity and are more dynamic on their faster growing plus ends; *in vivo,* most minus ends are anchored to MTOCs, while plus ends grow and shrink. Proper control of MT dynamics is essential for many MT dependent processes, including mitotic spindle assembly and function. Spindle MTs are very dynamic (Wadsworth and Salmon, 1986), and it has been observed that the addition of drugs that alter or inhibit MT dynamics disrupts spindle assembly and function (Toso et al., 1993, Jordan et al., 1992, Jordan et al., 1993). A better understanding of proteins that regulate MT dynamics in the cell may yield insights into the assembly and function of MT based structures.

A number of studies have focused on the regulation of dynamic instability. Factors that are known to influence dynamics include the nucleotide bound to tubulin and microtubule associated proteins (MAPs). MTs assemble from dimers of alpha and beta tubulin, each bound to one molecule of GTP. Subsequent to assembly, the GTP bound to the exchangeable site (E-site) on beta tubulin is hydrolyzed to GDP. Studies using a slowly hydrolyzable GTP analog (GMPCPP) have demonstrated that the hydrolysis of GTP is necessary for depolymerization (Hyman et al., 1992). The beta subunit is at the plus end of microtubules and the bound nucleotide can be exchanged on the polymer (Mitchison, 1993). Since the plus end is the dynamic end of MTs *in vivo* , this a likely point of regulation of MT dynamics in the cell. In a study designed to examine the role of GTP hydrolysis in MT dynamics, Davis et al. (1994) have mutated the region of yeast tubulin thought to bind GTP. Mutations in this region increase the rate of GTP hydrolysis by MTs, resulting in altered MT length distributions.

The prediction based on current models is that the catastrophe rate would be increased, however a more detailed study of one of these mutants employing video enhanced differential interference contrast (VEDIC) microscopy demonstrated a decrease in both growth and shrinkage rates, without much change in the catastrophe rates (Sage et al., 1995). It is possible that this decrease in growth rates is due to structural changes mutated tubulin subunits, or results from an increase in catastrophes and rescues that are below the resolution of light microscopy. When this mutant is expressed *in vivo,* it has a dominant effect of slowing progression through the cell cycle, again demonstrating that control of MT dynamics is essential for mitosis. In another study of the effect of the bound nucleotide on MT dynamics, Vandecandelaere et al. (1995) have altered the ratio of GTP tubulin to GDP tubulin *in vitro* with nucleoside-5'-diphosphate kinase (NDPK). The authors found that an increased ratio of GDP tubulin to GTP tubulin caused an increase in the critical concentration and an increase in the frequencies of catastrophe and rescue. Relatively small changes in the growth and shrinkage rates were observed. This is consistent with a model in which transitions are regulated by the nucleotide bound to the ends of MTs. However, no cellular regulators of MTs have been identified that modulate the rate of GTP hydrolysis by MTs or the nucleotide bound to tubulin subunits.

Recent studies have employed video microscopy to study the role of MAPs in modulating dynamic instability (for review see Hirokawa, 1994). Tau, a neuronal MAP, increases the rate of polymerization and decreases the frequency of catastrophe and the rate of depolymerization. Plots of catastrophe rates as a function of growth rate demonstrate that the catastrophe frequency is lowered more than would be expected simply from

increasing the growth rate. Phosphorylation of tau by MAP2 kinase affects all these activities independently and concentrations of phosphorlyated tau that have no effect on the growth rate still suppress catastrophes (Drechsel et al., 1992). Another study has demonstrated that unfractionated heat stable brain MAPs and purified MAP2 also increase the growth rate and lower the MT catastrophe frequency (Pryer et al., 1992). XMAP230 is a Xenopus MAP that is found in eggs, testes and tissue culture, but is apparently absent from non-dividing cells. This MAP has also been shown to increase the growth rate and suppress catastrophe frequencies and shrinkage rates. Phosphorylated XMAP230 fails to co-sediment with MTs (Andersen et al., 1994). MAP4 is the most abundant MAP in proliferating tissue culture cells. Video microscopy studies of MAP4 with purified MTs showed that unphosphorylated MAP4 increases the rescue frequency 30 fold, while having little effect on the other parameters of dynamic instability. Phosphorylation of MAP4 by $p34^{cdc2}$ decreases the rescue frequency 5 fold relative to the unphosphorylated MAP4 (Ookata et al., 1995). Thus, MAPs have been shown to stabilize MTs in their unphosphorylated form by suppressing catastrophes, increasing rescue and increasing growth rates.

MT dynamics are regulated throughout the cell cycle. Photobleaching studies demonstrated that MTs in interphase cells have longer half lives than MTs in mitotic spindles (Saxton et al., 1984, Salmon et al., 1984). Studies of individual MTs in interphase or mitotic *Xenopus* extracts have shown that the primary difference in dynamics is an increase in the catastrophe frequency in mitotic MTs (Belmont et al., 1990). Another study of MT dynamics in extracts of sea urchin eggs has shown that addition of okadaic acid to interphase extracts (to mimic mitotic phosphorylation states) causes a decrease in the rescue frequency (Gliksman et al., 1992).

Computer simulations of MT dynamics show that modulating either the catastrophe frequency, the rescue frequency, or both could account for the observed *in vivo* differences between interphase and mitotic MTs (Gliksman et al., 1993). Two MAPs found in dividing cells, MAP4 and XMAP230, are phosphorylated in mitosis and this phosphorylation lowers the MT stabilizing activity of these MAPs (Vandre et al., 1991, Hoshi et al., 1992, Andersen et al., 1994, Ookata et al., 1995). These MAPs may regulate cell cycle changes in MT dynamics by suppressing catastrophes and increasing rescue in interphase. However, the catastrophe frequency observed in cellular extracts (Belmont et al., 1990, Verde et al., 1992, Gliksman et al., 1992) and in cells (Cassimeris et al., 1988, Shelden and Wadsworth, 1993) is much higher than that observed *in vitro* with pure tubulin or tubulin plus MAPs (Walker et al., 1988, Drechsel et al., 1992, Pryer et al., 1992, Andersen et al., 1994, Ookata et al., 1995), suggesting that there are additional regulator of MT dynamics that actively increase the catastrophe rate.

A number of studies have sought to elucidate the upstream regulatory events that control MT dynamics during the cell cycle. The mitotic regulatory kinase $p34^{cdc2}$ associates with cyclins A and B in mitosis, and the $p34^{cdc2}$/cyclin B complex is essential for the mitotic specific changes in dynamic instability. In interphase Xenopus egg extracts, the addition of cyclin B, but not cyclin A, causes an increase in the catastrophe frequency of MTs (Verde et al., 1992). The model that $p34^{cdc2}$/cyclin B is the upstream regulator of MT dynamics is also consistent with intracellular localization studies showing that cyclin A is predominantly in the nucleus from S phase on, while cyclin B1 remains in the cytoplasm until the beginning of mitosis (Pines and Hunter, 1991). $p34^{cdc2}$/cyclin B associates with MT asters and

meiotic spindles in starfish oocytes (Ookata et al., 1993). Further studies in primate tissue culture cells presented strong evidence that $p34^{cdc2}$/cyclin B binds to MTs by interacting with MAP4, the most abundant MAP in these cells (Ookata et al., 1993). Addition of mitogen activated protein kinase (MAPK) to interphase extracts of Xenopus eggs can cause some changes microtubule length distributions (Gotoh et al., 1991), and changes in MT behavior follow changes MAP kinase activity, but not $p34^{cdc2}$ during meiosis in mouse oocytes (Verlhac et al., 1994). Thus, it is clear that $p34^{cdc2}$/cyclin B is one upstream regulator of cell cycle changes in MT dynamics and there may also be a role for MAP kinase in the regulation of MT dynamic parameters. MAPs are clearly one downstream target of these cell cycle regulators, however there is still a need for a downstream target that actively increases the catastrophe rate of MTs in a cell cycle dependent manner.

The work presented here focuses on the cell cycle regulation of MT dynamics. I describe i) the characterization of interphase and mitotic MT dynamics in *Xenopus* egg extracts, ii) the purification and characterization of a 17 kD protein that increases the catastrophe frequency of MTs *in vitro* and binds to tubulin dimers, and iii) the partial purification and characterization of a small molecular weight factor that increases the catastrophe frequency of MTs and destabilizes GMPCPP MTs.

REFERENCES

Andersen, S. S., Buendia, B., Dominguez, J. E., Sawyer, A., and Karsenti, E. (1994). Effect on microtubule dynamics of XMAP230, a microtubule-

associated protein present in Xenopus laevis eggs and dividing cells. J Cell Biol *127*, 1289-99.

Belmont, L. D., Hyman, A. A., Sawin, K. E., and Mitchison, T. J. (1990). Real-time visualization of cell cycle-dependent changes in microtubule dynamics in cytoplasmic extracts. Cell *62*, 579-89.

Cassimeris, L., Pryer, N. K., and Salmon, E. D. (1988). Real-time observations of microtubule dynamic instability in living cells. J Cell Biol *107*, 2223-31.

Davis, A., Sage, C. R., Dougherty, C. A., and Farrell, K. W. (1994). Microtubule dynamics modulated by guanosine triphosphate hydrolysis activity of beta-tubulin. Science *264*, 839-42.

Drechsel, D. N., Hyman, A. A., Cobb, M. H., and Kirschner, M. W. (1992). Modulation of the dynamic instability of tubulin assembly by the microtubule-associated protein tau. Mol Biol Cell *3*, 1141-54.

Gliksman, N. R., Parsons, S. F., and Salmon, E. D. (1992). Okadaic acid induces interphase to mitotic-like microtubule dynamic instability by inactivating rescue. J Cell Biol *119*, 1271-6.

Gliksman, N. R., Skibbens, R. V., and Salmon, E. D. (1993). How the transition frequencies of microtubule dynamic instability (nucleation, catastrophe, and rescue) regulate microtubule dynamics in interphase and mitosis: analysis using a Monte Carlo computer simulation. Mol Biol Cell *4*, 1035-50.

Gotoh, Y., Moriyama, K., Matsuda, S., Okumura, E., Kishimoto, T., Kawasaki, H., Suzuki, K., Yahara, I., Sakai, H., and Nishida, E. (1991). Xenopus M phase MAP kinase: isolation of its cDNA and activation by MPF. Embo J *10*, 2661-8.

Hirokawa, N. (1994). Microtubule organization and dynamics dependent on microtubule-associated proteins. Curr Opin Cell Biol *6*, 74-81.

Hoshi, M., Ohta, K., Gotoh, Y., Mori, A., Murofushi, H., Sakai, H., and Nishida, E. (1992). Mitogen-activated-protein-kinase-catalyzed phosphorylation of microtubule-associated proteins, microtubule-associated protein 2 and microtubule-associated protein 4, induces an alteration in their function. Eur J Biochem *203*, 43-52.

Hyman, A. A., Salser, S., Drechsel, D. N., Unwin, N., and Mitchison, T. J. (1992). Role of GTP hydrolysis in microtubule dynamics: information from a slowly hydrolyzable analogue, GMPCPP. Mol Biol Cell *3*, 1155-67.

Jordan, M. A., Thrower, D., and Wilson, L. (1992). Effects of vinblastine, podophyllotoxin and nocodazole on mitotic spindles. Implications for the role of microtubule dynamics in mitosis. J Cell Sci, 401-16.

Jordan, M. A., Toso, R. J., Thrower, D., and Wilson, L. (1993). Mechanism of mitotic block and inhibition of cell proliferation by taxol at low concentrations. Proc. Natl. Acad. Sci. *90*, 9552-56.

Mitchison, T., and Kirschner, M. (1984). Dynamic instability of microtubule growth. Nature *312*, 237-42.

Mitchison, T. J. (1993). Localization of an exchangeable GTP binding site at the plus end of microtubules. Science *261*, 1044-7.

Ookata, K., Hisanaga, S., Bulinski, J. C., Murofushi, H., Aizawa, H., Itoh, T. J., Hotani, H., Okumura, E., Tachibana, K., and Kishimoto, T. (1995). Cyclin B interaction with microtubule-associated protein 4 (MAP4) targets p34cdc2 kinase to microtubules and is a potential regulator of M-phase microtubule dynamics. J Cell Biol *128*, 849-62.

Ookata, K., Hisanaga, S., Okumura, E., and Kishimoto, T. (1993). Association of p34cdc2/cyclin B complex with microtubules in starfish oocytes. J Cell Sci *105*, 873-81.

Pines, J., and Hunter, T. (1991). Human cyclins A and B1 are differentially located in the cell and undergo cell cycle-dependent nuclear transport. J Cell Biol *115*, 1-17.

Pryer, N. K., Walker, R. A., Skeen, V. P., Bourns, B. D., Soboeiro, M. F., and Salmon, E. D. (1992). Brain microtubule-associated proteins modulate microtubule dynamic instability in vitro. Real-time observations using video microscopy. J Cell Sci *103*, 965-76.

Sage, C. R., Davis, A. S., Dougherty, C. A., Sullivan, K., and Farrell, K. W. (1995). beta-Tubulin mutation suppresses microtubule dynamics in vitro and slows mitosis in vivo. Cell Motil Cytoskeleton *30*, 285-300.

Salmon, E. D., Leslie, R. J., Karow, W. M., McIntosh, J. R., and Saxton, W. M. (1984). Spindle microtubule dynamics in sea urchin embryos. Analysis using fluorescence-labeled tubulin and measurements of fluorescence redistribution after laser photobleaching. J. Cell Biol. *99*, 2165-86.

Saxton, W. M., Stemple, D. L., Leslie, R. J., Salmon, E. D., Zavortink, M., and McIntosh, J. R. (1984). Tubulin dynamics in cultured mammalian cells. J. Cell Biol. *99*, 2175-86.

Shelden, E., and Wadsworth, P. (1993). Observation and quantification of individual microtubule behavior in vivo: microtubule dynamics are cell-type specific. J Cell Biol *120*, 935-45.

Toso, R. J., Jordan, M. A., Farrell, K. W., Matsumoto, B., and Wilson, L. (1993). Kinetic stabilization of microtubule dynamic instability in vitro by vinblastine. Biochemistry *32*, 1285-93.

Vandecandelaere, A., Martin, S. R., and Bayley, P. M. (1995). Regulation of microtubule dynamic instability by tubulin-GDP. Biochemistry *34*, 1332-43.

Vandre, D. D., Centonze, V. E., Peloquin, J., Tombes, R. M., and Borisy, G. G. (1991). Proteins of the mammalian mitotic spindle:

phosphorylation/dephosphorylation of MAP-4 during mitosis. J Cell Sci *98*, 577-88.

Verde, F., Dogterom, M., Stelzer, E., Karsenti, E., and Leibler, S. (1992). Control of microtubule dynamics and length by cyclin A- and cyclin B-dependent kinases in Xenopus egg extracts. J Cell Biol *118*, 1097-108.

Verlhac, M. H., Kubiak, J. Z., Clarke, H. J., and Maro, B. (1994). Microtubule and chromatin behavior follow MAP kinase activity but not MPF activity during meiosis in mouse oocytes. Development *120*, 1017-2.

Wadsworth, P., and Salmon, E. D. (1986). Microtubule dynamics in mitotic spindles of living cells. Ann N Y Acad Sci *466*, 580-92.

Walker, R. A., O'Brien, E. T., Pryer, N. K., Soboeiro, M. F., Voter, W. A., Erickson, H. P., and Salmon, E. D. (1988). Dynamic instability of individual microtubules analyzed by video light microscopy: rate constants and transition frequencies. J Cell Biol *107*, 1437-48.

Chapter 1

Real-Time Visualization of Cell Cycle–Dependent Changes in Microtubule Dynamics in Cytoplasmic Extracts

L. D. Belmont,* A. A. Hyman,† K. E. Sawin,* and T. J. Mitchison†
* Department of Biochemistry and Biophysics and
† Department of Pharmacology
University of California at San Francisco
San Francisco, California 94143

Summary

Using Xenopus egg extracts arrested in interphase or mitosis, we directly observed differences in microtubule dynamics at different stages of the cell cycle. Interphase extracts were prepared from eggs in the first interphase after meiosis. Mitotic extracts were prepared by addition of purified cyclin to interphase extracts. Microtubules were nucleated by the addition of centrosomes and visualized by fluorescence videomicroscopy in extracts to which rhodamine-labeled tubulin had been added. We found a striking difference in microtubule dynamics in mitotic versus interphase extracts. Quantitative analysis revealed that the rates of polymerization and depolymerization are similar in interphase and mitosis and that within the spatial and temporal resolution of our experiments the difference in dynamics is due almost entirely to an increase in the frequency of transition from growing to shrinking (catastrophe frequency) in the mitotic extracts.

Introduction

When cells progress from interphase to mitosis, large, relatively stable microtubule (MT) arrays are broken down and reorganized into much more dynamic mitotic spindles (for review, see Karsenti and Maro, 1986). The differences in MT organization and dynamics between interphase MT arrays and mitotic spindles have been probed in living cells by injection of fluorochrome-labeled or biotin-labeled tubulin subunits. Fluorescence recovery after photobleaching of fluorescent tubulin injected into cells showed that the rate of exchange of tubulin subunits between the monomer pool and MTs is very fast in mitotic cells and slower in interphase (Saxton et al., 1984; Salmon et al., 1984). MTs are very dynamic polymers; in vitro studies with purified tubulin (Mitchison and Kirschner, 1984a, 1984b; Horio and Hotani, 1986; Walker et al., 1988) have demonstrated that individual MTs alternate between prolonged phases of polymerization and depolymerization with abrupt, stochastic transitions between these two phases. This unique form of polymerization dynamics was termed dynamic instability to convey the idea that the MT lattice is inherently unstable unless it is actively polymerizing. It seemed likely that the differences in MT turnover rate between interphase and mitosis first observed by photobleaching corresponded to changes in dynamic instability behavior.

According to phenomenological models (Kirschner and Mitchison, 1986), dynamic instability can be characterized by four distinct rate constants: polymerization rate, depolymerization rate, rate of transition from growing to shrinking behavior (now termed catastrophe rate), and rate of transition from shrinking back to growing (rescue rate). These rates have all been determined for pure tubulin in vitro (Walker et al., 1988). Characterizing the dynamic instability rates that are altered during the cell cycle would provide a useful first step in understanding how MT dynamics inside cells are regulated at a molecular level.

Recently, MT turnover by dynamic instability has been observed directly on the periphery of interphase tissue culture cells by time-lapse videomicroscopy (Cassimeris et al., 1988; Schulze and Kirschner, 1988; Sammak and Borisy, 1988), and all four rates that govern dynamic instability have been determined. However, it has not thus far been possible to do this type of study in mitotic spindles because the MTs are too closely packed. Therefore, many questions are left unanswered: Can dynamic instability in fact occur at rates as fast as those inferred from photobleaching studies? If so, which of the rate constants are altered at the onset of mitosis? Finally, what is the molecular mechanism by which these rate constants are altered? To address these questions, an in vitro system would be useful because it could allow resolution of individual MTs displaying mitotic dynamics and would be amenable to subsequent biochemical studies.

Cytoplasmic extracts from Xenopus laevis eggs provide a good in vitro system for the study of the cell biology and biochemistry of the cell cycle (for review, see Lohka, 1989; Murray and Kirschner, 1989b). Extracts can be made that are arrested with the cytoplasm in interphase or mitotic states. These cytoplasmic states are determined by the activity of the MPF-p34^{cdc2} kinase. When this kinase is active, phosphorylation of multiple substrates is thought to keep the cytoplasm in a mitotic state. When it is inactive, the cytoplasm reverts to an interphase state, probably through the action of phosphatases.

In early Xenopus embryos, the levels of cyclin regulate the activity of MPF (Dunphy et al., 1988; Gautier et al., 1988; Lohka et al., 1988). Interphase and mitotic states of Xenopus egg extracts can be easily interconverted by appropriate manipulation of regulatory factors (Lohka and Masui, 1983; Lohka and Maller, 1985; Murray et al., 1989) or allowed to cycle autonomously (Murray and Kirschner, 1989a). Similar extracts have been used to study MT polymerization (Gard and Kirschner, 1987b, 1987a) and were shown to contain all of the proteins required to assemble multiple spindles in vitro (Lohka and Maller, 1985; K. E. S., unpublished data). Recent work by Verde et al. (1990) has shown that Xenopus extracts can be used to study the cell cycle regulation of MT dynamics. They observed MT polymerization by fixing MTs as a function of time after adding nucleating templates in interphase and mitotic extracts. It is difficult to determine the rate constants governing dynamic instability from this type of experiment, since catas-

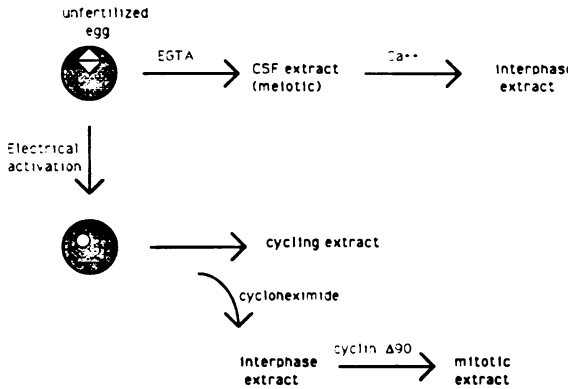

Figure 1. Preparation of Extracts with Defined Cell Cycle States

Interphase extracts were made by releasing unfertilized Xenopus eggs from their meiotic arrest by electrical activation. After preparing the extract, cycloheximide was added to prevent cyclin synthesis and thus entry into mitosis. Mitotic extracts were made by driving interphase extracts into mitosis by adding E. coli–expressed cyclin Δ90 protein. Cycling extracts were made in the same way as interphase extracts, but without adding cycloheximide. Meiotic extracts (CSF-arrested extracts) were made from unfertilized eggs in the presence of EGTA. These were driven into interphase by addition of Ca^{2+}.

trophe and rescue transitions cannot be directly observed. Determination of these rates requires real-time visualization of MT dynamics. In this work we added rhodamine-labeled tubulin to Xenopus egg extracts, allowing us to observe the behavior of individual MTs in real time in interphase and mitosis using fluorescence videomicroscopy.

Results

Visualization of Individual MTs in Extracts

We made concentrated cytoplasmic extracts from X. laevis eggs with determined cell cycle states. Extracts can be prepared in several different ways (Figure 1). For most of the experiments described we electrically activated eggs to release them from the meiosis II arrest, prepared extracts, and then added cycloheximide to the extract to inhibit protein synthesis. Such extracts are arrested in interphase since they are unable to synthesize cyclin protein, the synthesis of which is necessary and sufficient to drive these extracts into mitosis (Murray and Kirschner, 1989a; Minshull et al., 1989).

Mitotic extracts were derived from interphase extracts by the addition of an Escherichia coli–expressed, purified sea urchin cyclin B derivative from which 90 N-terminal amino acids have been deleted (cyclin Δ90). Cyclin Δ90 drives interphase extracts into mitosis and is not susceptible to the degradation of cyclin that is normally induced by entry into mitosis. Therefore, interphase extracts to which this cyclin is added become arrested in mitosis (Murray et al., 1989; M. Glotzer, unpublished data). Electrically activated extracts prepared in the absence of cycloheximide can go through several rounds of the cell cycle as a result of the activity of the endogenous cyclin (Murray and Kirschner, 1989a). These extracts are referred to as cycling extracts. Extracts made in the presence of EGTA maintain the natural meiosis II metaphase arrest by preserving the Ca^{2+}-sensitive activity cytostatic factor (CSF) (c-*mos* oncogene product) (Sagata et al., 1989; Noriyuka et al., 1989). These extracts could be induced to enter interphase by the addition of Ca^{2+}. For all types of extracts we assayed the cell cycle state of these extracts by observing nuclear morphology of added Xenopus sperm nuclei with Hoechst staining. In interphase extracts nuclei were rounded and the chromatin was decondensed. In mitotic extracts the nuclear envelope was disassembled and the chromatin was condensed (Lohka and Masui, 1983; see Figure 4).

To visualize single MTs in real time we added centrosomes purified from mammalian tissue culture cells to act as nucleating templates and tetramethylrhodamine-labeled bovine brain tubulin as a fluorescent tracer. The amount of tubulin added was equivalent to 25%–50% of the endogenous tubulin concentration in concentrated Xenopus extracts, which is 2–3 mg/ml (Gard and Kirschner, 1987a; our data not shown). Small aliquots of extract were squashed between a slide and a cover slip to provide a thin sample for observation by fluorescence videomicroscopy.

Two precautions were found to be essential to avoid photobleaching and photodynamic damage to the specimen: the mercury arc light source was dimmed using an aperture diaphragm and controlled by an electronic shutter to minimize the total light exposure of the specimen, and the extracts were supplemented with an oxygen scavenging enzyme system (Kishino and Yanagida, 1988). Sequential video images were collected at 5 or 2 s intervals. Individual MTs were observed polymerizing out from centrosomes, undergoing growing to shrinking transitions, and depolymerizing back to the centrosome.

Figure 2 shows sequential frames of MTs in an interphase extract (a) and an aliquot of the same extract after it has been driven into mitosis (b). We also observed MTs being released from the centrosome and translocating across the slide and centrosomes moving on the slide (Figure 2b). The most striking difference between MTs in the two cell cycle states was the decreased MT length in mitotic extracts.

Quantitation of Dynamics

To determine the difference in dynamic behavior between interphase and mitosis, MT lengths were measured as a function of time from sequences such as those shown in Figure 2. Figure 3 shows a graph of length vs. time for four typical interphase MTs measured at 5 s intervals and four typical MTs in a mitotic extract with frames taken at 2 s intervals. The rates of polymerization, depolymerization, catastrophe, and rescue were calculated from such data. A summary of measurements from three separate experiments is shown in Table 1. The last row on the table is an average of the three experiments shown. Growth rates revealed some variability between different extract preparations, but in all cases interphase growth rates were slightly slower than mitotic growth rates. Using the aggregate data, this difference in growth rate was statistically significant ($p = 0.01$). The large standard deviations for growth

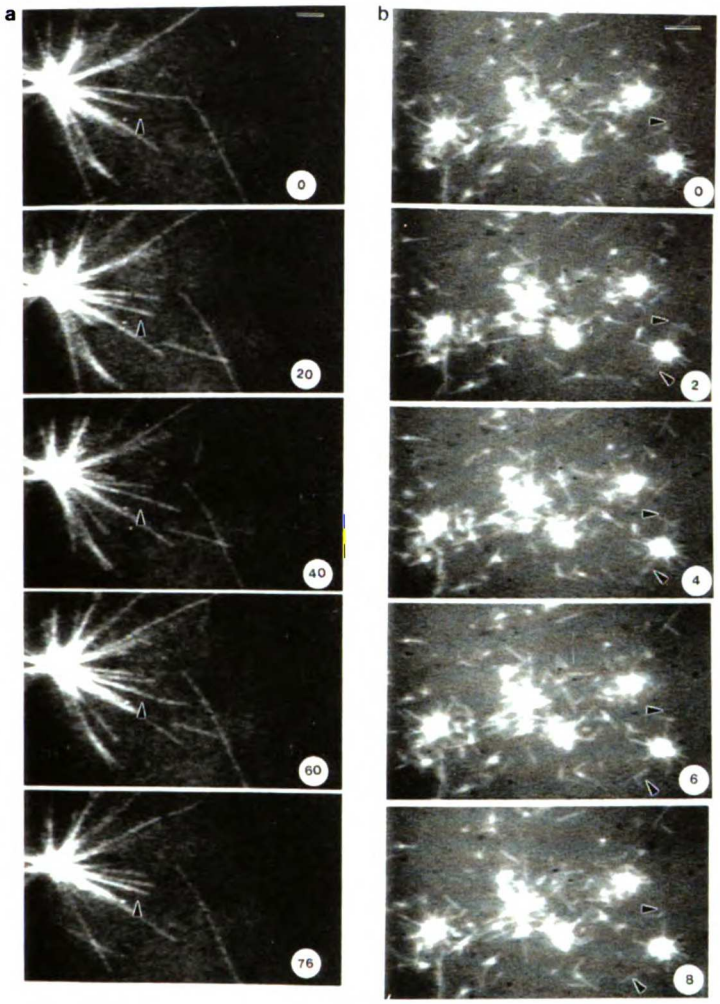

Figure 2. MTs Nucleated from Centrosomes in Interphase and Mitotic Extracts

MTs are visualized by the fluorescence of added bovine brain tubulin covalently modified with tetramethyl rhodamine.

(a) Sequential frames of an interphase extract containing centrosomes. The arrowheads mark the position of the end of a MT in the first frame. The MT end polymerizes past that point and then depolymerizes back toward the centrosome. Free MTs such as the two seen in this sequence are common in interphase extracts.

(b) Sequential frames from a mitotic extract. This is the same extract as (a) after it has been driven into mitosis by adding cyclin protein. The top arrowhead marks a stationary point, and a MT can be seen growing out to this mark and then shrinking back toward the centrosome. The centrosome itself moves upward slightly during this sequence. The lower arrowhead shows a MT that grows out from the centrosome, is released, and then translocates away. Most of the free MTs in mitotic extracts result from nucleation from centrosomes followed by release. The same number of centrosomes was added to interphase and mitotic extracts, and in (b) a field with a large number of centrosomes was chosen to demonstrate that all centrosomes on a cover slip behaved similarly. The bar represents 5 μm. The numbers indicate the time in s.

rates in a given experiment probably represent real differences in the rates at which particular MTs polymerize, as seen in previous studies in vivo (Schulze and Kirschner, 1988; Cassimeris et al., 1988). Shrinkage rates in both states of the extract are slightly faster than growth rates. The difference between shrinkage rates in the two different cell cycle states was not statistically significant ($p = 0.07$).

Because phase transitions appear to occur independently of the duration already spent in a particular phase (Walker et al., 1988), we could use data from all elongation phases to calculate catastrophe frequencies. To estimate catastrophe rate we measured how long the growth phase persisted for a number of MTs. The sum of these growth times was divided into the number of catastrophes observed in these MTs during the time of observation. The rescue rate was calculated in a similar manner. The primary difference in dynamics between the two cell cycle states is that the catastrophe rate is always much less in the interphase than in the mitotic extracts. There was no large or consistent difference between rescue rates in interphase and mitotic extracts. Within the spatial and temporal resolution of our system, the large difference in MT lengths between interphase and mitotic extracts is primarily due to the large difference in catastrophe rate.

Effects of Addition of Rhodamine Tubulin

We were concerned that the addition of rhodamine-labeled bovine brain tubulin might perturb the dynamic behavior of Xenopus MTs. We could not observe dynamics in real time in the absence of rhodamine tubulin but were able to take two approaches to determine whether there were perturbing effects on MT dynamics: fixation of MTs at steady-state in the presence and absence of rhodamine tubulin, and real-time observation of dynamics in varying amounts of rhodamine tubulin.

We incubated centrosomes in interphase extracts with varying amounts of rhodamine tubulin (0, 0.5, 1.0, and 2 mg/ml) for sufficient time to allow the MT length distribution to reach steady-state. We then fixed the MTs, sedimented them onto cover slips, and stained them with an anti-tubulin antibody. The conditions of incubation were identical to those used prior to real-time observation, ex-

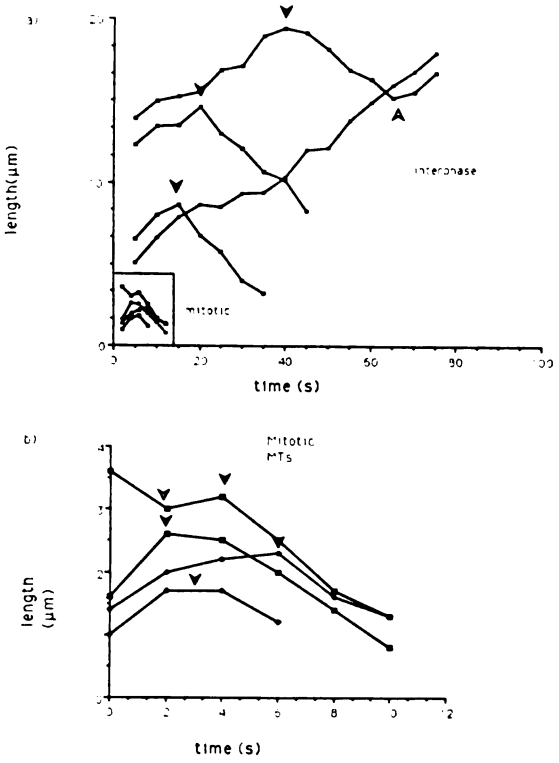

Figure 3. MT Length vs. Time

(a) Four typical MTs in interphase and mitotic extracts. Length of interphase MTs was measured every 5 s and length of mitotic MTs (boxed) was measured every 2 s.

(b) The mitotic MTs are shown on an enlarged scale for clarity. The black arrowheads mark catastrophes and the open arrowheads mark recoveries.

cept that the reaction was performed in polypropylene tubes rather than between a slide and cover slip. MT lengths measured from centrosomes under these conditions are shown in Table 2. For comparison, the last column on the table shows MTs measured from centrosomes used in a real-time study (experiment 3 in Table 1) where 1 mg/ml rhodamine tubulin was added. For both interphase and mitotic extracts we observed a decrease in mean length with increasing added rhodamine tubulin. However, the ratio between the mean interphase and mitotic lengths remains fairly constant. Thus, while addition of rhodamine tubulin does change MT behavior, it does not seem to change the basic difference between interphase and mitotic dynamics.

To determine the parameters affected by rhodamine tubulin, we added varying amounts of rhodamine tubulin (0.5, 1.0, and 2 mg/ml) to an interphase extract and observed MT dynamics with time-lapse videomicroscopy. Table 3 shows data averaged from two separate extract preparations. We observed only a very slight increase in rates of polymerization and no systematic change in rates of depolymerization as we increased the rhodamine tubulin concentration. However, we did observe an increase in catastrophe rate with increasing amounts of rhodamine tubulin. We were unable to carry out this experiment using mitotic extracts because the background was higher and visualization of individual MTs was possible only over a restricted range of rhodamine-tubulin concentrations. Since the ratio of mitotic to interphase lengths at steady-state (Table 2) is relatively constant over the whole range of rhodamine tubulin concentrations, it seems reasonable to assume that the main effect of rhodamine tubulin on mitotic dynamics is to increase catastrophe rate in a dose-dependent manner.

Taken together, the data in Tables 2 and 3 suggest that rhodamine tubulin does indeed perturb endogenous dynamic behavior, specifically by increasing catastrophe rate. This peturbation probably affects interphase and mitotic extracts in a similar way, and in any case is less than the basic difference between the two states. Thus, the artifacts introduced by the tracer molecule almost certainly do not affect our primary biological conclusion that the

Table 1. Polymerization, Depolymerization, Catastrophe, and Rescue Rates for Interphase and Mitotic MTs from Three Separate Experiments

Experiment	Cell Cycle State	Polymerization Rate (µm/min)	Depolymerization Rate (µm/min)	Catastrophe Rate (/s)	Rescue Rate (/s)
1	Interphase	11.1 ± 2.1 (n = 13)	15.2 ± 4.7 (n = 13)	0.031	0.016
	Mitotic	16.8 ± 2.4 (n = 7)	17.1 ± 5.4 (n = 9)	0.13	0.01
2	Interphase	8.6 ± 3.2 (n = 13)	12.3 ± 4.6 (n = 10)	0.013	0.009
	Mitotic	14.3 ± 6.6 (n = 9)	15.2 ± 4.7 (n = 13)	0.12	0.04
3	Interphase	8.5 ± 4.9 (n = 16)	16.6 ± 6.8 (n = 11)	0.01	0.009
	Mitotic	10.4 ± 6.2 (n = 29)	14.7 ± 6.0 (n = 29)	0.10	0.012
Average	Interphase	9.3 ± 4 (n = 42)	12.8 ± 6.0 (n = 34)		
	Mitotic	12.3 ± 6 (n = 45)	15.3 ± 5.6 (n = 51)		

All rates were calculated as described in the Experimental Procedures. The ± values are standard deviations. All experiments shown here are from electrically activated extracts with cycloheximide in the absence (interphase) or presence (mitotic) of cyclin Δ90. MTs were nucleated from CHO centrosomes. Rhodamine tubulin was added to 0.5 mg/ml in experiments 1 and 2 and to 1 mg/ml in experiment 3. The last row is an average of the data from the three experiments. The differences in polymerization rates between interphase and mitosis are slight but probably significant ($p = 0.01$) for the average of the three experiments. The difference in depolymerization rates between the two cell cycle states is not significantly different ($p = 0.07$). The major difference between the cell cycle states is the catastrophe rates.

Table 2. Mean Steady-State Lengths of MTs Nucleated from Centrosomes in Solution

	Polymerized in Solution				Polymerized under Time-Lapse Observation Conditions
Rhodamine Tubulin (mg/ml)	0	0.5	1	2	1
Interphase Length (μm)	40 (sd = 23)	31 (sd = 18)	23 (sd = 11)	12 (sd = 4)	19 (sd = 8)
Mitotic Length (μm)	16 (sd = 12)	11 (sd = 5)	6.2 (sd = 3)	5.2 (sd = 3)	4.0 (sd = 2)

The first four columns show measurements of mean lengths of MTs in an extract in interphase and mitosis in varying amounts of rhodamine tubulin. The centrosomes were added to extracts and incubated in polypropylene tubes for 10 min, fixed with glutaraldehyde, sedimented onto cover slips, and stained with an anti-tubulin antibody. The last column shows measurements of mean lengths measured from centrosomes during real-time observation (Table 1, experiment 3). Conditions of polymerization were identical for the real-time and fixed MT assays, except that the MTs from the real-time studies polymerized under the cover slip under periodic fluorescent illumination. All mean lengths are from measurement of at least 200 MTs from at least 8 different centrosomes. sd, standard deviation.

Table 3. Polymerizaiton, Depolymerization, and Transition Rates in Varying Rhodamine Tubulin Concentrations

Rhodamine Tubulin (mg/ml)	Polymerization Rate (μm/min)	Depolymerization Rate (μm/min)	Catastrophe Rate (/s)
2.0	10.9 (sd = 7.5, n = 18)	11.5 (sd = 5.4, n = 17)	0.053 (n = 18)
1.0	10.3 (sd = 5.3, n = 19)	19.6 (sd = 7.7, n = 20)	0.047 (n = 19)
0.5	8.5 (sd = 3.6, n = 22)	14.8 (sd = 6.1, n = 17)	0.021 (n = 22)

Measurements were taken as before, but over a 4-fold range of added tubulin concentration (0.5-2 mg/ml) in a Ca^{2+}-activated CSF extract. The data for all tubulin concentrations are averaged from measurements from two extract preparations.

principal difference between the two cell cycle states is that mitotic extracts have a higher catastrophe rate.

Extracts under Endogenous Cell Cycle Control

It is possible that a sea urchin cyclin derivative does not properly activate all of the mitotic activities in these extracts. To address this question, and to exclude the possibility that changes in MTs were due to artifacts from cycloheximide arrest or from other minor components contaminating the cyclin, we assayed MT dynamics in extracts where cell cycle changes were determined by endogenous cell cycle control proteins. Activated extracts were prepared in the absence of cycloheximide. Such extracts have been shown to undergo multiple rounds of the cell cycle as a result of the continued synthesis and period degradation of the endogenous cyclin (Murray and Kirschner, 1989a).

Two aliquots of a cycling extract were incubated in parallel. One contained Xenopus sperm nuclei and was used to assay for cell cycle state; the other contained centrosomes and rhodamine tubulin and was used to observe MT dynamics. Aliquots from the extract containing nuclei were taken every 20 min and fixed and stained with Hoechst. Aliquots for real-time observation of MT dynamics were taken every 5 to 10 min. The MT dynamics in aliquots taken from the extract during the first 30 min of incubation (Figure 4a) were typical of mitotic dynamics. This suggests that the extract had not yet progressed beyond the meiosis arrest at this time. At early time points sperm nuclei had not lost their elongated morphology (Figure 4d). Aliquots taken from the extract 40–70 min after the start of the incubation (Figure 4b) displayed typical interphase dynamics. During this interval the chromatin decondensed and the nuclei became round (Figure 4e). Aliquots taken after 70 min (Figure 4c) again showed typical mitotic dynamics. At these times the sperm chromatin had condensed and formed structures resembling mitotic chromosomes (Figure 4f). The changes in dynamics during the cell cycle were obvious upon video playback of the sequences; however, the fluorescence background in this particular experiment was too high to allow the resolution of single MTs necessary to obtain accurate quantitative data. It was clear that the changes in MT dynamics cycled in this extract in a manner that correlated well with changes in the cell cycle state assayed by nuclear morphology and that these dynamics were qualitatively similar to those observed in arrested extracts.

MT Translocation and Release from Centrosomes

During the course of these experiments, we noticed that MTs that were nucleated spontaneously or detached from centrosomes translocated across the slide. To analyze the polarity of movement in Xenopus extracts, MTs were nucleated from short stable MT seeds. These were made by polymerizing rhodamine-labeled tubulin in the presence of the nonhydrolyzable GTP analog GMPCPP (guanylyl-1(αβ) methylene diphosphonate). These MTs are stable to depolymerization in vitro (Hyman et al., 1990). MTs that polymerized in the extract could be distinguished from seeds because of the difference in fluorescence intensity (Figure 5). MTs polymerized from only one end of the GMPCPP seeds. Such polarized elongation was not unexpected, given the results of Allen and Borisy (1974), who showed that MTs polymerize from axonemes only at the plus end in cytoplasmic extracts, and those of Gard and Kirschner (1987a; 1987b), who demonstrated a similar phenomenon in Xenopus egg extracts.

Figure 5 shows three sequential frames at 2 s intervals of several MTs moving across a slide in a mitotic extract. These polarized MTs always moved along the substrate with the brightly labeled seed trailing; thus, the substrate is moving toward the MT minus end, and the motility is

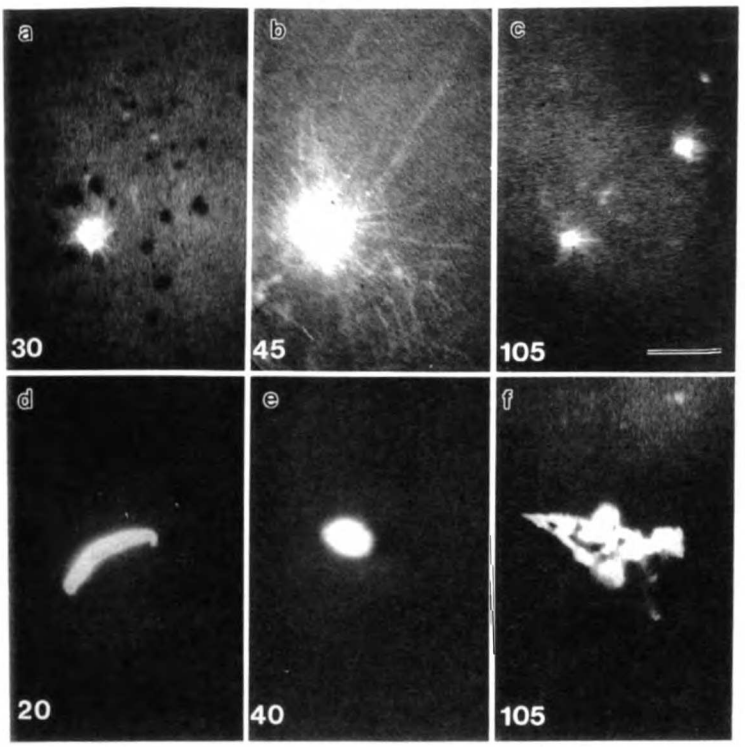

Figure 4. MT and Nuclear Morphology Cycling under Endogenous Cell Cycle Control in an Extract

MTs display meiotic (a), interphase (b), and mitotic (c) dynamics as the extract progresses through the cell cycle. (d)–(f) show nuclei incubated in parallel in an aliquot of the same extract. (d) Condensed sperm nuclei, (e) decondensed interphase nucleus, (f) condensed mitotic chromatin. The numbers are minutes after the start of incubation. The bar represents 10 μm.

minus end directed. We were able to confirm this by analyzing the movement of MTs that detached from the centrosome after polymerization. In these cases, a MT polymerized out from the centrosome, and therefore had a defined polarity with the plus end away from the centrosome (Mitchison and Kirschner, 1984b). In all of the cases examined, the MT moved away from the centrosome with its plus end leading. We therefore conclude that the polarity of the dominant motor activity that moves MTs in the extract is minus end directed.

To determine whether there was any difference in the rates of movement between interphase and mitosis, we measured rates of movement for ten MTs in both cell cycle states. For individual MTs the rate varied during the time observed, presumably because of blocking by other MTs and other factors. We therefore measured the peak rates of the MT movement and averaged them. The average peak rate was 1 μm/s. We found no significant difference between interphase and mitosis using this relatively crude assay.

The continuous detachment of MTs from centrosomes, which first drew our attention to the minus end–directed motility, is an interesting phenomenon in its own right. MTs were released much less frequently in interphase extracts than in mitotic extracts. To quantitate this difference, we counted the number of MTs released and the total number of nucleated MTs from centrosomes in several 30 s long sequences from interphase and mitotic extracts. Table 4 shows measurements of release for the three experiments shown in Table 1. Generally, we found that the rate of release of MTs per centrosome per second was greater in mitotic extracts. In all cases the rate of release of MTs per nucleated MT per second is higher in mitotic extracts.

We did not see an increase in the number of MTs nucleated per centrosome in miotic extracts, although it is known that mitotic maturation does increase the nucleating capacity of centrosomes in vivo (Kuriyama and Borisy, 1981).

Discussion

Xenopus Extracts as a Model System

By using Xenopus egg extracts as a source of cytoplasm with defined cell cycle states, we were able to observe directly the dynamic instability at mitotic rates for the first time and to compare directly the interphase and mitotic rates of polymerization, depolymerization, and transition. Attempts to visualize individual MTs in Xenopus extracts by transmitted light using dark-field or Nomarski optics were unsuccessful because vesicles and other cellular components obscured MTs. Because diluting or clarifying the extracts changed MT dynamic behavior, fluorescence was the only way we could observe MT dynamics in these extracts.

The use of fluorochrome-labeled tubulin as a tracer has two potential problems. Endogenous dynamics may be perturbed by the tracer molecule itself and also by photodynamic processes during illumination. We took three precautions to avoid photodynamic effects: first, the use of the relatively photostable fluorochrome tetramethyl-

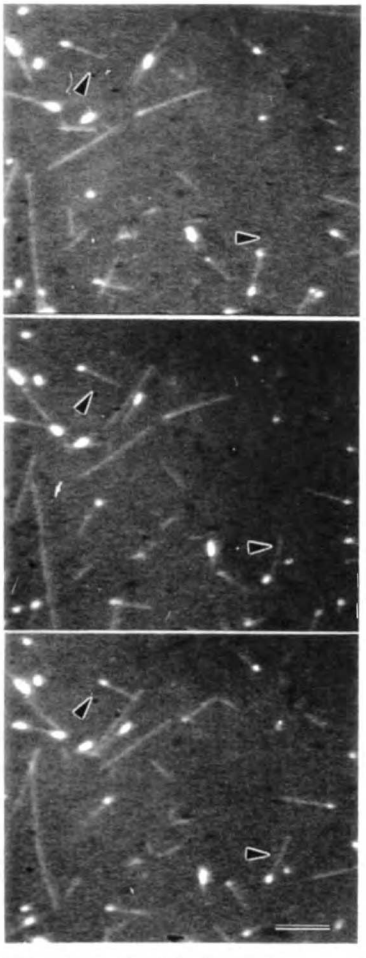

Figure 5. MT Translocating in a Mitotic Extract

Arrowheads mark stationary points on the slide, and the MTs can be seen to move in relation to these marks. Short stable seeds, polymerized from rhodamine tubulin in the presence of GMPCPP, were added to a mitotic extract. They elongate on their plus ends with Xenopus tubulin mixed with rhodamine tubulin. The seed is visible as a bright dot at the minus end of each MT. Note that MTs move with the seed trailing. The frames are taken at 2 s intervals. The bar represents 5 μm.

rhodamine; second, scavenging oxygen by using the enzyme system of Kishino and Yanagida (1988); and third, limiting the total light dose using shuttering and an aperture diaphragm. Using these precautions, photodynamic damage was greatly inhibited, allowing several minutes of observation.

Comparisons of MTs polymerized in solution in the absence of fluorescent excitation with MTs polymerized while being observed by fluorescence suggest that there are not major effects on MTs from photodynamic events under our conditions of observation (Table 2). Comparing columns 3 and 5 in Table 2 we note that MT polymerization under a cover slip does give mean lengths that are 20%–30% shorter than those for MTs fixed in solution under the same solution conditions. We suspect that this may be due to adsorbtion of protein onto the glass slide and cover slip given the high surface area to volume ratio. We do not think that the difference is due to photodynamic effects, since no change of mean MT length with time was observed for several minutes of observation of a given centrosome using the videomicroscope. Because the difference in mean MT length between solution and cover slip is much less than the difference between interphase and mitosis, we do not think that this technical consideration affects our conclusion that the principle difference between the two cell cycle states is the catastrophe rate. The use of the oxygen scavenging system was absolutely essential, and photodynamic effects were evident after only a few images in its absence. Thus, most of the readily observable photodynamic events are probably mediated by oxygen radicals in our system.

We found that the rhodamine-labeled bovine brain tubulin does affect endogenous dynamics, primarily by increasing the catastrophe rate in a dose-dependent manner. Preliminary experiments suggest that this difference may be due in part to the use of bovine tubulin (which prefers a higher temperature for polymerization), since addition of unlabeled bovine tubulin also causes a dose-dependent decrease in mean MT lengths (data not shown). Since the effects on interphase and mitotic dynamics are similar, the perturbation introduced by the probe does not invalidate our principal conclusion.

Table 4. Release of MTs from Centrosomes in Interphase and Mitotic Extracts

Experiment	Cell Cycle State	Number of Centrosomes	Number of MTs	MTs/Centrosome	Release/Centrosome (x10exp-2/s)	Release/MT (x10exp-3/s)
1	Interphase	6	181	30	6	2
	Mitotic	4	50	12.5	6.7	5
2	Interphase	3	52	17.3	1	0.64
	Mitotic	9	70	7.8	5	6.2
3	Interphase	5	95	19	0	0
	Mitotic	10	105	10.5	7	6.7
	Interphase	14	328	23.4	2.8	1.2
Average	Mitotic	23	225	9.8	6.1	6.2

Release rates were measured for the three experiments shown in Table 1. Rates of release were calculated from measurements of total nucleated MTs and total number of MTs released in several 30 s sequences.

Regulation of Dynamic Instability during the Cell Cycle

We found that MTs nucleated from centrosomes exhibit dynamic instability when the cytoplasm is in both interphase and mitotic states. The actual values that we obtained for polymerization and depolymerization rates in interphase are in reasonable agreement with rates determined for interphase in amphibian tissue culture cells: polymerization rate of 7.2 μm/min, depolymerization rate of 17.3 μm/min, catastrophe rate of 0.014/s, and rescue rate of 0.044/s (Cassimeris et al., 1988). This suggests that our in vitro system does provide a reasonable model for in vivo MT dynamics. We do not, however, expect the actual values that we obtained for the four dynamic instability rates to be exactly the same as those inside living Xenopus embryos for several reasons: our procedures entailed a 25% dilution of cytoplasm, and we added exogenous components including the oxygen scavenging enzymes and sucrose from the centrosome buffer. We also do not know how much peturbation is introduced by the egg lysis procedure. Thus, our experiments should not be taken as an attempt to determine in vivo rates, but rather as a model system to try to determine the molecular basis for the regulation of MT dynamics during the cell cycle.

We found that MTs turn over much more rapidly in the mitotic extracts compared with interphase, and this change is due almost entirely to an increase in catastrophe rate in mitosis. The other parameters of dynamic instability—polymerization, depolymerization, and rescue rates—change little between the two cell cycle states. The dynamic instability we have observed takes place at rates sufficient to account for the rapid MT turnover seen in mitotic cells by photobleaching and other techniques.

It is interesting to compare our conclusions with those of Verde et al. (1990), who also used Xenopus extracts in defined cell cycle states to examine MT dynamics. The important difference in the studies is that Verde et al. assayed dynamics by adding centrosomes and then fixing at various time points and staining with anti-tubulin antibodies. This allowed them to observe MT length without adding exogenous probes. However, they were not able to observe catastrophe and rescue events or to measure polymerization and depolymerization rates directly. Like us, Verde et al. observed a cell cycle–dependent difference in mean length at steady-state, with longer MTs in interphase extracts (20 μm) and shorter MTs in mitotic extracts (7–12 μm). They also estimated initial elongation rates of 18 μm/min for interphase and 3.8 μm/min for mitosis, and suggested that polymerization rate is regulated during the cell cycle, a conclusion with which we disagree. Part of the discrepancy may arise from the use of a high speed supernatant in the Verde et al. study. More important, the "elongation" rate measured by Verde et al. is actually a composite rate of the four dynamic instability parameters. Differences in catastrophe alone could easily account not only for differences in steady-state length but also for differences in measured elongation rate even at early time points.

A second important difference was that in the work of Verde et al., the extracts were warmed immediately before adding centrosomes, so that there was little spontaneous polymer present during initial polymerization rate measurements. Our studies were conducted at steady-state, i.e., in the presence of a steady-state level of spontaneous polymer. Like Verde et al., we found that there was more spontaneous polymer present in the interphase extracts, which accounts for the lower fluorescent background we found in interphase. Thus, there was probably more tubulin monomer present during their determination of interphase polymerization rate than there was in our study. This probably accounts for the higher rate they obtain. We think that the steady-state rate is likely to be closer to physiological conditions.

Mechanisms for Regulating MT Dynamics

The changes in MT dynamics we observed between interphase and mitosis could be regulated at many levels. Because the changes occur in the presence of cycloheximide, they must be due to posttranslational events. We think it unlikely that a change in Ca^{2+} level is responsible, because our extracts were buffered and contained EGTA. At present we cannot rule out changes in pH. However, we suspect the dynamics are more likely to be regulated by mitosis-specific phosphorylation of proteins that interact with MTs. Phosphorylation is responsible for changing the properties of several other proteins whose functions change between interphase and mitosis (Lohka et al., 1987; Karsenti et al., 1987), and recent studies have shown that MT dynamics can be regulated directly by phosphatases (Verde and Karsenti, personal communication).

Given our current understanding of dynamic instability, increased transition rate in mitotic extracts could be due to three factors: a decrease in effective monomer concentration, a factor acting directly at the ends of MTs causing transitions, or a change in factors acting along the length of MTs.

Studies using pure tubulin have shown that lowering of tubulin monomer concentration lowers polymerization rate and increases catastrophe rate of MTs (Walker et al., 1988). We observe that the polymerization rate is in fact increased slightly in mitotic extracts (where catastrophe rate is higher) and, furthermore, that the lack of spontaneous polymer and increased fluorescent background in mitotic extracts suggest that monomer concentration is if anything higher in mitosis. Thus, the MT turnover rate in these extracts is not regulated simply by tubulin monomer concentration. This rules out models that postulate that MT turnover in mitosis is accelerated by a decrease in monomer concentration caused by increased numbers of nucleating sites (Mitchison and Kirschner, 1987).

The second model involves modulation of MT dynamics by factors that act on plus ends. This could involve transient capping of the polymer, or perhaps increase in the GTP hydrolysis rate of the MT end in mitosis. These models are the most attractive because they could explain a change in catastrophe rates without a change in polymerization and depolymerization rates, which would be consistent with our data. Although no factors that interact with MT ends have been characterized thus far, there is no reason to think they will not be found. The only protein cur-

rently known to interact with the ends of growing MTs is tubulin itself.

The third model proposes that the catastrophe rate is changed by factors such as microtubule-associated proteins (MAPs) that act along the length of a MT. This type of model is attractive because MAPs affect MT dynamics in other systems. Furthermore, XMAP, the dominant polymerization promoting factor in Xenopus eggs, undergoes mitosis-specific phosphorylation (Gard and Kirschner, 1987b, 1987a), which could influence its polymer stabilizing activity. On theoretical grounds, if XMAP stabilizes MTs in interphase by binding to the polymer lattice, and if this stabilization is reduced by phosphorylation in mitosis, then we would expect to see a faster depolymerization rate in mitosis. In fact, our data show little difference in depolymerization rate between interphase and mitosis. This argues against a MAP as the primary regulator of differences in dynamics. On the other hand, the fact that we see little change in polymerization rate in mitosis may be misleading in that steady-state monomer concentration is probably higher in mitosis because of the lack of spontaneous nucleation (see above). Thus, specific polymerization rate, i.e., polymerization rate divided by tubulin monomer concentration, may in fact be lower in mitosis. Because the primary effect of interphase XMAP is to stimulate polymerization rate, this may argue in favor of a role for XMAP in regulating dynamics during the cell cycle.

MT Motility and Release from Centrosomes

Translocation of MTs across the cover slip in extracts is probably due to cytoplasmic dynein, because the motility is minus end directed and inhibited by low vanadate concentrations (data not shown). We saw no significant difference in translocation rates between interphase and mitotic extracts, but more subtle differences in motility factors could exist. Xenopus extracts may prove to be a useful system for studying the involvement of motor proteins in mitosis.

In our experiments MTs were released from centrosomes in both mitotic and interphase extracts, but more frequently in mitotic extracts. Release of the MTs occurs at the centrosome, almost never from breaks in the middle of the MT. The MTs then move away from the centrosome, presumably due to minus end–directed motors in the extract that have absorbed to the slide. It is unclear why MTs are released more frequently in mitotic extracts, but the two most likely possibilities are an increase in activity or accessibility of MT motor molecules resulting in more frequent pulling of MTs off the centrosome or a change in the nucleating properties or minus end binding of the centrosome itself. Release of MTs from centrosomes may have interesting physiological consequences. It has been proposed that MTs are released from centrosomes at the onset of mitosis in sea urchin embryos (Harris et al., 1980) and Dictyostelium amoebae (Kitanishi-Yumura and Fukui, 1987). MTs also seem to be released at the centrosome during reorientation of chromosomes that are mono-oriented (Ault and Nicklas, 1989). Release of MT minus ends from centrosomes may turn out to play an important role in spindle dynamics, and Xenopus extracts should be a useful system to study this phenomenon.

Experimental Procedures

Preparation of Extracts

Electrically activated extracts were prepared from X. laevis eggs as described (Murray and Kirschner, 1989a) with the modification that for interphase-arrested extracts, the 15 min ice bath incubation before the crushing spin was omitted and cycloheximide was added to 100 μg/ml to the cytoplasmic layer immediately after it was collected. Cycling extracts were prepared in the same way except that the cycloheximide was omitted. Extracts were kept on ice and used within a few hours of preparation. It was found that freezing or incubating extracts on ice for more than 5 hr caused the catastrophe rate of MTs in mitotic extracts to decrease. Attempts to clarify the extract by using a high speed supernatant gave inconsistent results and also decreased the mitotic catastrophe rate.

To drive electrically activated cycloheximide-arrested extracts into mitosis, 1 μl (~5 μg of protein) of E. coli–expressed purified sea urchin cyclin Δ90 (M. Glotzter and M. Kirschner, unpublished data) was added to 50 μl of extract. Ten microliters of this was mixed with Xenopus sperm nuclei and incubated at 20°C to determine the time necessary for the extract to form condensed chromatin. The remainder of the extract was incubated for the same length of time in the absence of nuclei. Once chromatin had condensed in the test aliquot, the extract was used for observation of mitotic dynamics. For observation of interphase dynamics extracts were either observed within 5 min of cyclin addition or extract buffer was added instead of cyclin.

Meiotically arrested extracts (CSF) were prepared as described (Murray et al., 1989). They were driven into interphase by the addition of 1/40 vol of 16 mM $CaCl_2$, 100 mM KCl, 1 mM $MgCl_2$ and 1/50 vol of 5 mg/ml cycloheximide, incubation for 30 min at 20°C, and incubation on ice for 5 min in the presence of 1/40 vol of 16 mM EGTA. Mock activations were identical except that the incubation buffer contained no $CaCl_2$.

Chinese hamster ovary centrosomes were prepared as described (Mitchison and Kirschner, 1986). Tetramethylrhodamine-labeled tubulin and stable MT seeds were prepared as described (Hyman et al., 1990).

Observation of Dynamics

Samples (20 μl) of an extract in a defined cell cycle state were mixed with 1 or 2 μl of 10 mg/ml rhodamine tubulin and 2 μl of either centrosomes or stable MT seeds. These mixtures could be kept at 20°C for up to 1 hr, after which time the visualization of MTs deteriorated. Samples (5 μl) were taken from these and mixed with 0.5 μl of 10× anti-fade (2 mg/ml catalase, 4 mg/ml glucose oxidase, 0.5 M glucose, and 40 mM DTT), and 1 μl samples were squashed under a 22 × 22 mM no. 1 cover slip, sealed with molten beeswax, and observed within 15 min. It was found that prolonged incubation with this anti-fade system caused MTs to aggregate, although no obvious effects on dynamics at short incubation times (less than 30 min) were observed. The microscope stage was kept at 22–23°C.

Fixed MT Assays

An extract was prepared, incubated after addition of cyclin Δ90 or buffer, and assayed for cell cycle state by observing the condensation state of sperm nuclei added to a test aliquot. Four microliters of centrosomes were added to 40 μl of the extract in each cell cycle state. This was split into four tubes to which were added 1 μl of bovine brain rhodamine tubulin at 20, 10, or 5 mg/ml in IB (50 mM K glutamate, .5 mM $MgCl_2$ [pH 7]), or 1 μl of IB . These were then incubated at 23°C for 10 min. Samples (1 μl) were taken and immediately fixed in 100 μl of .5% glutaraldehyde, .4% TX-100 in BRB80 (80 mM K PIPES, 1 mM $MgCl_2$, 1 M EGTA [pH 6.8]). This was sedimented onto cover slips, fixed in methanol, and stained with the anti-tubulin antibody DM1α as described (Mitchison and Kirschner, 1986). Two hundred MTs were measured for each condition for calculation of mean length.

Video Microscopy

All recording was performed on a Zeiss universal microscope equipped with a broad band rhodamine filter set (Ex 510–560 nm, Em 590 LP) and an Olympus DPlanapo 1.4× objective. Images were collected

with a SIT camera (COHU) using an 8 × eyepiece, passed through a Maxvision AT1 image processor (Datacube) for digitization and eight-frame averaging, and recorded using a Panasonic OMDR. Shuttering of the fluorescence excitation light was essential to avoid photobleaching, and averaging, shutter control, and recording were coordinated using custom-written software. Images were recorded every 2 s for most mitotic sequences and every 5 s for most interphase sequences. The shutter was opened for the minimum length of time required to collect eight images (0.25 sec). In addition, an aperture diaphragm in the epi-illumination tube was used to reduce the excitation light level to the minimum required for single MT imaging. Images were collected from a single field until a detectable decrease in fluorescence intensity indicated that photobleaching had occurred (typically 50 frames). After this point, but not before, we began to observe occasional breaks in the middle of MTs and fragmentation of centrosomes, which we took as evidence for photodynamic damage. MT polymerization rates determined from the first in-focus frames of a given field, and those determined from frames taken just before photobleaching became detectable, were not significantly different. The actual number of frames that could be collected before photodamage occurred was quite variable between different extract preparations, but interphase and mitotic extracts showed no systematic difference in this respect.

Data Analysis

MT lengths were measured by displaying each frame on a video monitor and moving a cursor along the length of the MT measuring from the edge of the centrosome to the end of the MT using JAVA software (Jandel Video Systems Analysis). The minimum length resolvable by this system is ~0.6 μm. MTs that were released were not used for measurement of dynamics because of the difficulty in distinguishing growth from motility. MTs were measured in every frame to generate the graphs of MT lifetimes. In most experiments MT polymerization and depolymerization rates were calculated from two frames in a given phase in which the ends were clearly defined. Transitions were quite apparent in sequences played back at video rates, even in cases where the end was not always clearly defined in each frame. Catastrophe rates are calculated by dividing the number of transitions from growing to shrinking by the total time spent in the growing phase. Rescue rates are the number of transitions from shrinking to growing divided by the time spent in the shrinking phase. The resolution of the camera was 0.25–0.38 μm (2–3 pixels). Accuracy of measurement was within .26 μm as estimated by repeated measurement of a mitotic MT.

Acknowledgments

We wish to thank Andrew Murray for cell cycle advice and psychological counseling, and Marc Kirschner and Cynthia Kenyon as well as Andrew Murray for critical reading of the manuscript. We also thank M. Glotzer for providing cyclin Δ90 and advising us on its preparation. This work was supported by grant #RO1-GM39565 from the National Institutes of Health and fellowships from the Packard Foundation and Searle Foundation (T. J. M.), the National Science Foundation (L. D. B.), and the Markey Foundation (A. A. H.).

The costs of publication of this article were defrayed in part by the payment of page charges. This article must therefore be hereby marked "*advertisement*" in accordance with 18 U.S.C. Section 1734 solely to indicate this fact.

Received February 13, 1990; revised April 24, 1990.

References

Allen, C., and Borisy, G. (1974). Structural polarity and directional growth of *Chlamydomonas flagella*. J. Mol. Biol. *90*, 381–402.

Ault, J. G., and Nicklas, R. B. (1989). Tension, microtubule rearrangements, and the proper distribution of chromosomes in mitosis. Chromosoma *98*, 33–39.

Cassimeris, L., Pryor, N. K., and Salmon, E. D. (1988). Real-time observations of microtubule dynamic instability in living cells. J. Cell Biol. *107*, 2223–2231.

Dunphy, W. D., Brizuela, L., Beach, D., and Newport, J. (1988). The Xenopus *cdc2* protein is a component of MPF, a cytoplasmic regulator of mitosis. Cell *54*, 423–431.

Gard, D. L., and Kirschner, M. W. (1987a). Microtubule assembly in cytoplasmic extracts of *Xenopus* oocytes and eggs. J. Cell Biol. *105*, 2191–2201.

Gard, D. L., and Kirschner, M. W. (1987b). A microtubule-associated protein from *Xenopus* eggs that specifically promotes assembly at the plus-end. J. Cell Biol. *105*, 2203–2215.

Gautier, J., Norbury, C., Lohka, M., Nurse, P., and Maller, J. (1988). Purified maturation-promoting factor contains the product of a Xenopus homolog of the fission yeast cell cycle control gene *cdc2+*. Cell *54*, 433–439.

Harris, P., Osborn, M., and Weber, K. (1980). Distribution of tubulin-containing structures in the egg of sea urchin *Strongylocentrotus purpuratus* from fertilization through first cleavage. J. Cell Biol. *84*, 668–678.

Horio, T., and Hotani, H. (1986). Visualization of the dynamic instability of individual microtubules by dark-field microscopy. Nature *321*, 605–607.

Hyman, A., Drechsel, D., Kellogg, D., Salser, S., Sawin, K., Steffen, P., Wordeman, L., and Mitchison, T. (1990). Preparation of modified tubulins. Meth. Enzymol., in press.

Karsenti, E., and Maro, B. (1986). Centrosomes and the spatial distribution of microtubules in animal cells. Trends Biochem. Sci. *11*, 460.

Karsenti, E., Bravo, R., and Kirschner, M. (1987). Phosphorylation changes associated with the early cell cycle in *Xenopus* eggs. Dev. Biol. *119*, 442–453.

Kirschner, M., and Mitchison, T. (1986). Beyond self-assembly: from microtubules to morphogenesis. Cell *45*, 329–342.

Kishino, A., and Yanigida, T. (1988). Force measurements by manipulation of a single actin filament. Nature *334*, 74–76.

Kitanishi-Yumura, T., and Fukui, Y. (1987). Reorganization of microtubules during mitosis in *Dictyostelium*: dissociation from MTOC and selective assembly/disassembly in situ. Cell Motil. Cytoskel. *8*, 106–117.

Kuriyama, R., and Borisy, G. G. (1981). Microtubule nucleating activity of centrosomes in CHO cells is independent of the centriole cycle but coupled to the mitotic cycle. J. Cell Biol. *91*, 822–826.

Lohka, M. (1989). Mitotic control by metaphase-promoting factor and *cdc2*. J. Cell Sci. *92*, 131–135.

Lohka, M. J., and Maller, J. L. (1985). Induction of nuclear envelope breakdown, chromosome condensation, and spindle formation in cell-free extracts. J. Cell Biol. *101*, 518–523.

Lohka, M. J., and Masui, Y. (1983). Formation in vitro of sperm pronuclei and mitotic chromosomes induced by amphibian ooplasmic components. Science *220*, 719–721.

Lohka, M. J., Kyes, J. L., and Maller, J. L. (1987). Metaphase protein phosphorylation in *Xenopus laevis* eggs. Mol. Cell. Biol. *7*, 760–768.

Lohka, M., Hayes, M., and Maller, J. (1988). Purification of maturation promoting factor, an intracellular regulator of early mitotic events. Proc. Natl. Acad. Sci. USA *85*, 3009–3013.

Minshull, J., Blow, J. J., and Hunt, T. (1989). Translation of cyclin mRNA is necessary for extracts of activated Xenopus eggs to enter mitosis. Cell *56*, 947–956.

Mitchison, T. J. (1989). Polewards microtubule flux in the mitotic spindle: evidence from photoactivation of fluorescence. J. Cell Biol. *109*, 637–652.

Mitchison, T. J., and Kirschner, M. W. (1984a). Dynamic instability of microtubule growth. Nature *312*, 237–242.

Mitchison, T. J., and Kirschner, M. W. (1984b). Microtubule assembly nucleated by isolated centrosomes. Nature *312*, 232–236.

Mitchison, T. J., and Kirschner, M. W. (1986). Isolation of mammalian centrosomes. Meth. Enzymol. *134*, 261–268.

Mitchison, T. J., and Kirschner, M. W. (1987). Some thoughts on the partitioning of tubulin between monomer and polymer under conditions of dynamic instability. Cell Biophys. *11*, 35–55.

Mitchison, T., Evans, L., Schultze, E., and Kirschner, M. (1986). Sites of microtubule assembly and disassembly in the mitotic spindle. Cell *45*, 515–527.

Murray, A., and Kirschner, M. (1989a). Cyclin synthesis drives the early embryonic cell cycle. Nature *339*, 275–280.

Murray, A. W., and Kirschner, M. W. (1989b). Dominoes and clocks: the union of two views of the cell cell cycle. Science *246*, 614–621.

Murray, A., Solomon, M., and Kirschner, M. (1989). The role of cyclin synthesis in the control of maturation promoting factor activity. Nature *339*, 280–286.

Noriyuka, S., Daar, I., Oskarssou, M., Showalter, S., and Vande Woude, G. (1989). The product of the *mos* oncogene as a candidate "initiator" for oocyte maturation. Science *245*, 643–646.

Sagata, N., Watanabe, N., Vande Woude, G. F., and Ikawa, Y. (1989). The c-*mos* proto-oncogene is a cytostatic factor responsible for meiotic arrest in vertebrate eggs. Nature *342*, 512–518.

Salmon, E. D., Leslie, R. J., Karow, W. M., McIntosh, J. R., and Saxton, R. J. (1984). Spindle microtubule dynamics in sea urchin embryos. Analysis using fluorescence-labeled tubulin and measurements of fluorescence redistribution after laser photobleaching. J. Cell Biol. *99*, 2165–2174.

Sammak, P. J., and Borisy, G. G. (1988). Direct observation of microtubule dynamics in living cells. Nature *332*, 724–726.

Saxton, W. M., Stemple, D. L., Leslie, R. J., Salmon, E. D., Zavortink, M., and McIntosh, J. R. (1984). Tubulin dynamics in cultured mammalian cells. J. Cell Biol. *99*, 2175–2186.

Schulze, E., and Kirschner, M. W. (1986). Microtubule dynamics in interphase cells. J. Cell Biol. *102*, 1020–1031.

Schulze, E., and Kirschner, M. W. (1988). New features of microtubule behavior *in vivo*. Nature *334*, 356–359.

Verde, F., Labbé, J., Dorée, M., and Karsenti, E. (1990). Regulation of microtubule dynamics by *cdc2* protein kinase in cell-free extracts of *Xenopus* eggs. Nature *343*, 233–238.

Walker, R. A., O'Brien, E. T., Pryer, N. K., Sobeiro, M. F., Voter, W. A., Erickson, H. P., and Salmon, E. D. (1988). Dynamic instability of individual microtubules analyzed by video light microscopy: rate constants and transition frequencies. J. Cell Biol. *107*, 1437.

Chapter 2

Identification of a Protein that Binds Tubulin Dimers and Increases the Frequency of Catastrophes in Microtubules

Lisa D. Belmont* and Timothy J. Mitchison

UCSF Department of Biochemistry and Biophysics/
Cellular and Molecular Pharmacology
San Francisco, CA 94143-0448

* Author for Correspondence

Dept. of Biochemistry box 0448
513 Parnassus
University of California, San Francisco
San Francisco, CA 94143-0448

SUMMARY

We have purified a 17.2 kD protein that binds tubulin dimers and increases the catastrophe frequency of microtubules *in vitro*. Sequence analysis identified this protein as Op18/Stathmin, a conserved phosphoprotein that is phosphorylated in response external signals and is highly expressed in leukemia cells. This is the first identification of a microtubule regulator that responds to external signals and is up regulated in cancer cells. Op18/Stathmin is also the first physiological microtubule regulator that preferentially binds unpolymerized subunits. This molecule is a good candidate for a regulator that causes the increased MT catastrophe rate observed in mitosis.

INTRODUCTION

Microtubules (MTs) are essential for a number of cellular processes, including intracellular transport, maintenance of cell shape, cell polarity and mitosis. *In vitro,* MT polymers interconvert between phases of slow growth or rapid shortening, with abrupt transitions between the two phases (Mitchison and Kirschner, 1984). Growth and shrinkage are due to addition or loss of tubulin subunits from the ends of MTs, respectively. Transitions from growing to shrinking are called catastrophes and transitions from shrinking to growing are called rescues. This behavior, termed dynamic instability, has been observed with pure tubulin (Hotani, 1986, Walker et al., 1988), in cellular extracts (Belmont et al., 1990, Gliksman et al., 1992), and *in vivo* in many cell types (Cassimeris et al., 1988, Shelden and Wadsworth, 1993). Microtubules have an intrinsic

polarity and are more dynamic on their faster growing plus ends. *In vivo,* most minus ends are anchored to MT organizing centers (MTOCs), while plus ends grow and shrink. Proper control of MT dynamics is essential for many MT dependent processes, including mitotic spindle assembly and function. Spindle MTs are very dynamic (Wadsworth and Salmon, 1986), and drugs that alter or inhibit MT dynamics disrupt spindle assembly and function (Amin and Wadsworth, 1991, Jordan et al., 1992, Jordan et al., 1993).

MT dynamics are regulated during the cell cycle. Photobleaching studies demonstrated that MTs in interphase cells have longer half lives than MTs in mitotic cells (Salmon et al., 1984, Saxton et al., 1984), and studies of individual MTs in interphase or mitotic *Xenopus* extracts have shown that the primary difference between these two cell cycle states is an increase in the catastrophe frequency of mitotic MTs (Belmont et al., 1990). Another study of MT dynamics in extracts of sea urchin eggs has shown that addition of okadaic acid to interphase extracts (to mimic mitotic phosphorylation states) causes a decrease in the rescue frequency (Gliksman et al., 1992). Computer simulations of MT dynamics suggest that modulating either the catastrophe frequency, the rescue frequency, or both could account for the observed *in vivo* differences between interphase and mitotic MTs (Gliksman et al., 1993).

The best characterized cellular factors that regulate MT dynamics are microtubule associated proteins (MAPs), which have been identified because they co-purify with MTs through several rounds of polymerization (for review see Hirokawa, 1994). Video microscopy studies of the effect of MAPs on MT dynamics have shown that they stabilize MTs by increasing the rate of polymerization, suppressing catastrophes, or increasing rescues

(Drechsel et al., 1992, Pryer et al., 1992, Shiina et al., 1992, Andersen et al., 1994, Ookata et al., 1995). Two prominent MAPs found in dividing cells, MAP4 and XMAP230, are phosphorylated in mitosis and this phosphorylation lowers the MT stabilizing activity of these MAPs (Vandre et al., 1991, Andersen et al., 1994, Ookata et al., 1995). These studies suggest that MAP phosphorylation during mitosis may regulate MT dynamics by inactivating the stabilizing influence of MAPs. However, the catastrophe frequency observed in cellular extracts and in cells is much higher than that observed *in vitro* with pure tubulin or tubulin plus MAPs. This suggests that there are additional regulators of MT dynamics that actively increase the catastrophe frequency.

A number of studies have sought to elucidate the upstream regulatory events that control MT dynamics during the cell cycle. The mitotic regulatory kinase $p34^{cdc2}$ associates with cyclins A and B in mitosis, and the $p34^{cdc2}$/cyclin B complex is required for the mitotic specific changes in dynamic instability. In interphase *Xenopus* egg extracts, the addition of cyclin B, but not cyclin A, causes an increase in the catastrophe frequency of MTs (Verde et al., 1992). $p34^{cdc2}$/cyclin B associates with MT asters and meiotic spindles in starfish oocytes (Ookata et al., 1993), and further studies in primate tissue culture cells presented strong evidence that $p34^{cdc2}$/cyclin B binds to MTs by interacting with MAP4, the most abundant MAP in these cells (Ookata et al., 1995). Addition of mitogen activated protein kinase (MAPK) to interphase extracts of Xenopus eggs can also cause some changes in microtubule dynamics (Gotoh et al., 1991), and changes in MT behavior follow changes in MAP kinase activity, but not $p34^{cdc2}$ activity during meiosis in mouse oocytes (Verlhac et al., 1994). These studies suggest that $p34^{cdc2}$/cyclin B is one upstream regulator of cell cycle

changes in MT dynamics and that there may also be a role for MAP kinase in the regulation of MT dynamics in the cell cycle.

While recent work has greatly increased our knowledge of cell cycle dependent regulation of MT dynamics, none of these studies has identified a MT regulator that causes the increased mitotic catastrophe frequencies observed *in vivo*. In this study we set out to directly identify cellular factors that increase the catastrophe rate of MTs.

RESULTS

The Assay

Our previous work demonstrated that catastrophe frequency is the primary parameter of MT dynamics regulated during the cell cycle. In order to study the mechanism by which catastrophe frequency is regulated, we designed assays to identify cellular factors that increase the frequency of microtubule catastrophes. The primary, rapid assay was designed to identify any factors that destabilize MTs. This assay will not distinguish factors that destabilize MTs by increasing the catastrophe frequency from those that destabilize MTs by increasing the depolymerization rate or inhibiting assembly. Therefore, at various stages of purification we characterized fractions further by observing their effect on MT dynamics using video-enhanced differential interference contrast (VEDIC) microscopy to test whether the fractions of interest did indeed increase the catastrophe frequency.

We chose calf thymus as a tissue source because it contains many dividing cells and provides a large amount of starting material. For the

rapid assay, we added fractions from a cellular extract prepared from calf thymus to tubulin (mixed 4:1 with rhodamine labeled tubulin), GTP, and axonemes, to nucleate MT assembly, and incubated at 37°C. Aliquots were taken after 15 and 20 minutes and placed on a slide for observation with fluorescence microscopy. A high speed supernatant (HSS) of the calf thymus extracts inhibited MT assembly in this assay, and similar results were obtained in preliminary fractionation of *Xenopus* egg extracts. Figure 1 shows MT assembly in a buffer control compared to a partially purified active fraction.

Purification of a Microtubule Destabilizing Activity

Extracts of calf thymuses were subjected to the fractionation steps shown in table 1. An SDS PAGE gel of the active fractions through the first four purification steps is shown in figure 2. We determined that at least one destabilizing activity is present after incubation of the HSS at 100°C for 15 minutes, which proved to be an excellent purification step (see table 1). The largest difference in MT lengths between the boiled HSS and buffer was observed at a pH of 7.5 with a $MgCl_2$ concentration of 5mM, and Pipes is best buffer for MT assembly. Subsequently, all assays were carried out in AB (80 M K Pipes pH 7.5, 5mM $MgCl_2$, 1mM EGTA).

Treating the boiled HSS with trifluoroacetic acid (TFA) and acetonitrile resulted in no loss of activity. Therefore, we were able to use reverse phase C18 chromatography to further purify the activity. Prior to loading the boiled HSS onto the C18 column, we precipitated the activity with 80% MeOH. The precipitation caused an apparent loss of specific activity; however, it tripled the amount of extract that we could resolve on

the C18 column, presumably due to removal of MeOH soluble compounds that bind to the C18 column. Peaks from multiple C18 columns were then pooled, re-loaded onto the C18 column and eluted with a shallow gradient of acetonitrile with 0.12% TFA. The activity consistently eluted at 32.5% acetonitrile. When analyzed by SDS PAGE this fraction contained one major protein around 17 kD and between 0 and 8 minor bands by Coomassie and silver staining. The major band in these preparations is 17,220 daltons (sd=1.65) by mass spectometry. All fractions that had been purified in this manner were pooled and used for subsequent characterization. This fraction will be referred to in the text as the 2X C18 fraction.

To determine if a protein was responsible for the activity, we used α lytic protease to digest the proteins in the 2X C18 fraction. Activity was completely lost after incubation with the protease and subsequent inhibition of protease activity. This inactivation of destabilizing activity was a result proteolysis since the fraction was fully active after incubation with protease that had been pre-incubated with its inhibitor (see figure 3).

One additional purification step was necessary to determine which polypeptide was responsible for the activity. Figure 4A shows a gel of the region around which the activity elutes from a C18 column. The active fractions were pooled and fractionated on a sizing column. The peak of activity co-eluted with the peak of the 17.2 kD protein (figure 4, B and C). We measured gel band intensity to confirm that the 17.2 kD band was the only band detectable by coomassie staining that peaked in intensity with the peak of MT destabilizing activity (figure 4C). Subsequent silver staining of the gel revealed no other proteins with an intensity peak that coincided with the activity peak (data not shown). The 17.2 kD protein eluted from the sizing

column in the position expected for a 20 kD protein, indicating it is probably a globular monomer.

We used this sizing column fraction to estimate stoichiometry of the purified protein to tubulin. The protein concentration in this fraction is 0.03 μg/μl. If we make the assumption that all of the protein in the fraction is in the 17.2 kD band, we calculate that the concentration of this protein in our rhodamine tubulin assays is 1.2μM in conditions that inhibit approximately half of the MT assembly (1U/μl). The concentration of tubulin dimers is 32 μM, giving a stoichiometry of one Op18 molecule for every 27 tubulin dimers for half maximal activity.

The Destabilizing Factor Increases the Microtubule Catastrophe Frequency

We used the 2X C18 fraction for functional characterization. We measured MT assembly at various concentrations of the active fraction with tubulin, GTP, and axonemes until we found a concentration that allowed enough MT assembly to measure dynamics, but still had a clear inhibitory effect. This concentration was approximately 0.8 units/μl in 15 to 20 μM tubulin in the presence of axonemes. We flowed the tubulin mix into a pre-warmed chamber and recorded MT dynamics in the presence of the activity at 35.5 ^{o}C. We measured the growth rate and the catastrophe frequency for individual MTs at each tubulin concentration. The data, shown in table 2, reveal that incubation with this concentration of active fraction results in a slight decrease in the growth rate and a 5 to 10 fold increase in the catastrophe frequency. Comparison of conditions with similar growth rates demonstrates that incubation with the active fraction increases the catastrophe frequency more than would be expected simply from lowering

the growth rate. We were unable to get a good measurement of average depolymerization rate because we recorded only a small number of shrinking microtubules. However, in the data we analyzed we see no consistent change in the depolymerization rate with the active fraction. We did not observe enough rescue events to assess any effect on rescue frequency.

Using an estimate of 0.03 μg of protein/unit activity (from the sizing column fraction) we estimate the stoichiometry of tubulin dimers to the 17.2 kD protein in these assays to be 14:1 in 20 μM tubulin and 11:1 in 15 μM tubulin. Addition of twice as much active fraction to 20 μM tubulin inhibits nearly all MT assembly. These stoichiometries are lower than those observed to cause similar effects in our rhodamine tubulin assay. This is consistant with previous observations (Belmont et al., 1990) that rhodamine tubulin causes MTs to be less stable.

The 17.2 kD Protein Binds Tubulin Dimers

We had previously found no depletion of the MT destabilizing activity when we depleted *Xenopus* extracts of MTs and MAPs (data not shown). Since the destabilizing activity did not seem to have a high affinity for MTs we tested it's ability to bind unpolymerized tubulin dimers. We mixed equimolar amounts of tubulin and the 2X C18 fraction in the absence of GTP and analyzed the mixture by gel filtration chromatography. When these proteins were run separately on this column, tubulin eluted at 14.5' and the 17.2 kD protein eluted at 18.6'. However, when these proteins were mixed, all the detectable 17.2 kD protein eluted entirely with tubulin (see fig 5A). There are no other proteins in the tubulin preparation detectable by

Commassie staining. Therefore, it is unlikely that proteins other than tubulin are present in sufficient amounts to account for the shift in elution time of the 17.2 kD protein. Due to the large amount of dilution on the column, we were unable to detect any of the minor proteins in the 2XC18 fraction in this experiment. Tubulin dimers and the 2XC18 fraction were mixed at 15μM each, and more than 90% of the factor bound to tubulin under these conditions. Quantitation of gel band intensities reveals that the first fraction of tubulin to elute from the sizing column co-elutes with less 17.2 kD protein than the subsequent fractions. This suggests that binding Op18 may actually slow tubulin's mobility in the gel filtration column. The finding that 17.2 kD protein binds to tubulin further argues that it is the protein responsible for the observed effects on MT dynamics in our video microscopy experiments.

We next tested the ability of the protein to bind taxol stabilized MTs under the same conditions. Fig 5B shows that the 17.2 kD protein remains with the unpolymerized fraction of the tubulin when the 2X C18 fraction is added to taxol stabilized MTs. Lane (a) shows that the majority of the 17.2 kD protein is in the supernatant with the unpolymerized tubulin and the amount in the pellet is equivalent to the amount that pellets in the absence of MTs (lane c). When the 2X C18 fraction is added prior to taxol addition, it inhibits the polymerization of MTs by taxol (compare the tubulin in the pellet in lanes b and d).

Identification of the 17.2 kD Protein as Op18/Stathmin

We used the peak fraction from one C18 column to determine peptide sequence of the 17.2 kD protein. In this preparation the 17.2 kD band was the

only band visible on a silver stained SDS gel. This protein was blotted onto a PVDF membrane for protein sequencing and we obtained sequence from two separate peptides. These sequences, HEAEVLK and IEENNNFSK, both showed 100% identity to a previously identified phosphoprotein named oncoprotein18 (Op18), p19, prosolin, leukemia associated protein 18 (lap18), or stathmin (Braverman et al., 1986, Schubart et al., 1987, Hanash et al., 1988, Sobel et al., 1989). The predicted MW of the human protein is 17,172 Da (Curmi et al., 1994) compared to our measured MW of 17,220 for the bovine protein. Therefore, we concluded that the 17.2 kD protein we have characterized is identical to this protein which we will refer to in the text as Op18.

DISCUSSION

In this study we have purified a small heat stable protein that increases the MT catastrophe frequency *in vitro*. Since observed catastrophe rates *in vivo* are much higher than those observed *in vitro* and are increased even more in mitosis, we think this protein may be involved in the regulation of MT catastrophe frequencies in cells and may increase catastrophes in mitosis. This is the first identification of a physiological regulator of MT dynamics that preferentially binds unpolymerized tubulin dimers, suggesting novel mechanisms of action. The loss of activity upon purification suggests that there may be other MT destabilizers in cells. Recent work by Walczak et al. (submitted) has identified a kinesin related protein (XKCM1) as a protein that may increase the catastrophe frequency of MTs. These two proteins are the first "catastrophe factors" to be identified.

We purified Op18 by an activity assay that identified MT destabilizing factors, and then assayed for the ability to increase catastrophe frequency. By analyzing MTs with video microscopy techniques, we determined that the purified fraction both increased catastrophes and decreased the growth rate in a concentration dependent manner. If one decreases the MT growth rate by lowering tubulin concentration there is an increase in catastrophe frequency (Walker et al., 1988). However, our data demonstrate that the increase in catastrophe frequency with Op18 exceeds the increase expected simply from lowering the growth rate. At similar growth rates with and without Op18, the catastrophe frequency is three to six fold higher with Op18. We also know from our stoichiometry estimates that Op18 is not increasing catastrophes simply by binding tubulin dimers and making them unavailable for assembly. One Op18 molecule for every 27 tubulin dimers will inhibit approximately half of the MT assembly in our rhodamine tubulin assay, and lowering the tubulin concentration by 1/27 will not have such a dramatic effect.

The finding that Op18 binds to unpolymerized tubulin suggests that it acts by a different mechanism from other known physiological regulators of MT dynamics. MAPs, the best characterized physiological regulators of MT assembly, bind to polymerized MTs and stabilize the lattice. A number of drugs bind to tubulin dimers in well characterized sites and inhibit assembly (for reviews see Correia, 1991, Sackett, 1995), and it has long been speculated that there is a physiological regulator of MTs that binds to these sites *in vivo*. Op18 is a good candidate for this type of regulator and it will be interesting to test if Op18 competes for any of these binding sites. Although these drugs inhibit MT assembly at high concentrations, drugs that have been studied in detail do not increase the catastrophe frequency (Toso

et al., 1993), suggesting a different mechanism of action than Op18. There are several models that could account for the observed effect that Op18 has on MT catastrophe rates. Op18 and tubulin dimers are likely to form a complex in the cell. This tubulin/Op18 complex could then add on to MT ends and increase the probability of a catastrophe by either blocking further addition of subunits, increasing the rate of GTP hydrolysis by tubulin subunits, or causing structural changes in the MT lattice that favor depolymerization.

The identification of Op18 as a regulator of MT catastrophe rates may shed new light on the data concerning the role of Op18 in proliferating and cancerous cells. Op18 has been identified as a protein that is highly expressed in acute leukemia (Hanash et al., 1988) and as a protein that is phosphorylated in response to external signals (Sobel et al., 1989). Until now there has been no candidate for a regulator of MT dynamics that responds to external signals or a MT regulator associated with malignancy. Op18 is phosphorylated in response to agents that promote cellular proliferation (for review see Sobel, 1991) and its expression is increased in proliferating cell types (Rowlands et al., 1995). Increased Op18 expression in rapidly dividing cells is consistent with our hypothesis that Op18 is required for establishment of mitotic MT dynamics. Previous studies of Op18 have identified four sites that are phosphorylated *in vivo*. Of these four, S25 was found to be a very good substrate for MAP kinase and S38 a good substrate for p34cdc2 in *vitro* (Marklund et al., 1993, Beretta et al., 1993). Since cell cycle dependent changes in MT catastrophe rates are known to be downstream of $p34^{cdc2}$/cyclin B and possibly MAP kinase, Op18 is a plausible target of these kinases and the downstream effector responsible for regulating MT dynamics. Expression of Op18 genes in which the serines

at the 25 and 38 position have been changed to alanine results in a block in G2/M with about 2/3 of the cells arresting in G2 and 1/3 arresting in mitosis. The mitotically arrested cells have condensed chromosomes that appear aggregated instead of aligned on a metaphase plate (Marklund et al., 1994). Antisense expression of Op18 and expression of Op18 with all the phosphorylation sites mutated to alanine result in a similar phenotype (Marklund et al., 1994, Larsson et al., 1995, Luo et al., 1994). The phenotype of the mitotically blocked cells is quite interesting when considered in the context our studies. Taxol, a drug that suppresses MT dynamics at low concentration and promotes MT assembly at high concentrations, causes a mitotic block when added to cells. Taxol concentrations that suppress MT dynamics *in vitro*, block cells at metaphase with chromosomes that fail to align on the metaphase plate (Jordan et al., 1993). Thus, the mitotic block resulting from Op18 inhibition is consistent with a role in regulating MT dynamics in mitosis. The G2 arrest is more difficult to interpret in this context. This arrest suggests a checkpoint blocking progression of the cell cycle; however, the known cell cycle checkpoints that monitor MT assembly respond to absence of proper spindle formation and block exit from mitosis (Murray, 1994, Hartwell and Kastan, 1994). This suggests that there may be another role for Op18 prior to M phase, or an as yet unidentified MT dependent checkpoint.

It has been known for some time that MTs are much more dynamic in mitosis than in interphase, and that this is largely due to a increase in the catastrophe frequency and a decrease in rescue frequency in mitosis. Studies on the effect of MAPs on MT dynamics suggest that the decrease in rescue frequency could be due to inactivation of MAPs by phosphorylation during mitosis. MAPs stabilize MTs, increase rescues, or suppress catastrophes *in*

vitro in their unphosphorylated form. These MAPs are phosphorylated in mitosis *in vivo,* and the phosphorylated forms fail to suppress catastrophes or increase rescues due to a lowered affinity of phosphorylated MAPs for MTs. However, these studies do not answer the question of how the catastrophe frequency is actively increased in mitosis. We propose that Op18, a protein that increases the catastrophe frequency of MTs *in vitro,* is a likely mediator of the increased frequency of catastrophes in mitosis. Thus, cell cycle regulation of MT dynamics would consist of phosphorylation of MAPs, resulting in a lower rescue frequency and activation of Op18 resulting in an increased catastrophe frequency.

EXPERIMENTAL PROCEDURES

Rhodamine Tubulin Assays

Bovine brain tubulin was purified by several cycles of assembly and disassembly and flowed over a phosphocelluose column to remove MAPs. Bovine brain tubulin and tetramethyl rhodamine labeled tubulin were mixed at a ratio of 4:1 unlabeled to labeled. The tubulin was mixed with GTP, axonemes, and a fraction from calf thymus to a final concentration of 3.5 mg/ml tubulin and 2mM GTP. All components were in assay buffer (AB), 80mM KPipes pH 7.5, 5mM $MgCl_2$, 1mM EGTA, and all manipulations up to this point were performed at 4°C. 10 µl of this mix was incubated at 37°C, 2 µl aliquots were taken at 15 and 20 minutes, diluted into 50 µl of 60% glycerol and mixed by gently pipetting up and down 3 times with a cut off pipette tip. 2.3 µl of this mix was placed on a glass slide, covered with a 18X18 mm coverslip and observed on a Zeiss Standard microscope with a

rhodamine filter set. One unit of activity per μl was defined as the fold dilution of fraction at which more than 50% inhibition of MT assembly was observed in this assay.

The pH optimum was determined by exchanging the boiled HSS into 80 mM K Pipes, 5mM $MgCl_2$, 1mM EGTA at pH increments of 6.8, 7.1, 7.3, and 7.5 using 1 ml P-4 (BioRad) spin columns.

Purification

Fetal calf thymuses that had been quick frozen in liquid nitrogen and shipped on dry ice were purchased from AnTech (Tyler, Texas). Extracts were prepared by breaking up the frozen thymus with a hammer and homogenizing the frozen pieces in a chilled Waring blender with AB (80 M K Pipes pH 7.5, 5mM $MgCl_2$, 1mM EGTA) + 1mM PMSF and 0.1% 2-Mercaptoethanol (2-ME) at 1-2 mls per gram of thymus. The crude extract was centrifuged in a GSA rotor at 10,000 rpm for 20 minutes and the supernatant was filtered through 6 layers of cheesecloth into a chilled beaker. This low speed supernatant was centrifuged at 4°C for 4.5 hours at 50,000 rpm in a Beckman 50.2 Ti rotor or for 18 hours at 19, 000 rpm in a Beckman type 19 rotor. The resultant supernatant is referred to as the high speed supernatant (HSS) in the text.

2-ME was added to the HSS to a final concentration of 1% and the HSS was placed in a boiling water bath for 20 minutes. The boiled HSS was cooled on ice and centrifuged for 15 minutes at 10,000 rpm at 4°C. The supernatant was collected and 5 volumes of methanol (Fisher, Optima grade) was added to precipitate the protein. After chilling overnight at -20°C, the

protein was sedimented for 15 minutes at 10,000 rpm at 4°C in a GSA rotor and the pellet was briefly dried under vacuum.

The pellet from 25 to 35 mls of HSS was dissolved in 2 to 4 mls of milli-Q purified water and spectrophotometric grade trifluoroacetic acid (TFA) was added to a final concentration of 1%. The sample was filtered through a 2μm spin filter (Millipore) and loaded onto a preparative C18 column (Vydac 218TP510) that had been pre-equilibrated with 0.12% TFA. The column was washed with 0.12% TFA and eluted with a gradient of 25 to 35 % acetonitrile with 0.12% TFA over 40 minutes at 4mls/min. 1.6 ml fractions were collected and 350 μl of each was dried overnight under vacuum. These dry fractions were dissolved in AB and assayed as described above. The activity consistently eluted at 32.5% acetonitrile. Active fractions were pooled and re-fractionated over the same C18 column. The pooled active fractions from the second C18 column, referred to in the text as 2X C18 fraction, were dissolved in AB and frozen in 20 μl aliquots at -80°C.

For gel filtration, active fractions from the first C18 column were pooled, dissolved in a minimal volume of AB, and loaded onto a sizing column (Supelco G3000PWXL) that had been equilibrated with AB containing 0.1% 2-ME. The column was run at 0.5 ml/min. and 200μl fractions collected. These were assayed directly or after concentration in a Millipore 10,000 NMWL Ultrafree-MC filter unit. Ovalbumin, chymotrypsinogen and profilin were used as size standards.

Protein concentration in crude fractions was measured using BioRad Bradford reagent, and in more purified fractions was measured using the absorbance at 220.

Observation of Microtubule Dynamics

Video-enhanced DIC (VEDIC) analysis was performed on a Zeiss axioplan microscope with a 63X PlanApo 1.4NA objective. Images were collected with a Hamamatsu C2400 video camera connected to an Argus 10 image processor, for background subtraction and contrast enhancement, and recorded on super VHS tapes with a Panasonic AG1960 SVHS VCR.

2X C18 fractions (8 Units/μl) were diluted 10 fold into a mix of tubulin, 2mM GTP and axonemes in AB. This mixture was kept on ice until observation. Flow chambers were constructed by placing two strips of double sided tape on a coverslip and covering with an 18X18 mm coverslip. The flow chamber was warmed to 37°C and 10 μl of tubulin at the same concentration being used in the assay was flowed into the chamber. This was then wicked out and replaced with the tubulin, axonemes, GTP, and 2X C18 fraction mixture. The chamber was sealed with VALAP (1:1:1 Vaseline: lanolin: paraffin) and placed on a warmed microscope stage for observation. The stage was kept at 35.5°C +/- 0.5°C by wrapping the objective and condenser lenses with Silastic tubing and flowing warm water through the tubing. The MTs in each flow chamber were observed for approximately 15'. MT growth rates were determined by measuring the length of an individual MT at time intervals ranging from 3 to 20 seconds when the plus end was clearly in focus. The slope of a line obtained by linear regression of length versus time was used as the growth rate. The catastrophe frequency was calculated by dividing the total number of catastrophes by the total time MTs were observed in the growth phase.

Protease Digestion

20 µls of 2X C18 purified fraction was thawed and diluted with an equal volume of AB. 9 µl of fraction, or AB alone, was mixed with 1 µl of either α–lytic protease or 1µl of α–lytic protease that had been pre-incubated with the inhibitor, 2-aminoethyl benzene sulfonyl fluoride (AEBSF, Calbiochem). The digestion reactions were incubated at 37°C for 50' and 1 µl of AEBSF at 10mM was added to samples that did not have AEBSF added at the start. Samples were chilled on ice for 5' and assayed as described above or added to SDS sample buffer for electrophoresis.

Tubulin Binding and Quantification of Gel Bands

Tubulin and the 2X C18 fraction were mixed in an equimolar ratio (150 pmoles of each) in 20 µl of AB and incubated for 10' at 37°C. This mix was then loaded onto a sizing column (Supelco G3000PWXL) that had been equilibrated with AB and the column was eluted at 0.5 ml/min. at 20 °C. 400 µl fractions were collected and 20 µl of each fraction was analyzed by SDS PAGE on a 15% gel. Tubulin alone and 2X C18 alone were analyzed in parallel under similar conditions. The tubulin preparation was MAP free as determined by coomassie staining of an SDS polyacrylamide gel.

To test binding of the 17.2 kD protein to stabilized MTs, we made taxol MTs as follows. 10 µl of 30µM tubulin and 1µl of 30 µM taxol were incubated for 10' at 37°C, 1µl of 300µM taxol was added, and the mix was incubated for another 10'. We then added 10µl of 30µM 2X C18 fraction to the taxol MTs, incubated for an additional 10' at 37°C, layered the mixture onto a 25µl cushion of 60% glycerol and sedimented in a TLA100 rotor for 5' at 100K. The supernatant and pellet were collected and added to SDS sample buffer for PAGE analysis. To test the effect of pre-addition of the purified fraction,

we added 10μl of 30μM 2XC18 fraction before addition of taxol and incubated for 20' after addition of 300μM taxol.

Gel band intensity was measured by scanning a coomassie stained SDS gel on a UMAX PowerLook Scanner into a Macintosh 7100/80 AV computer. The intensity of the bands in the scanned image was measured using the gel plotting macro in NIH Image.

Protein Sequencing

The active fraction was separated on a 15% SDS gel and blotted onto PVDF membrane as described (Matsudaira, 1993). The band 17.2 kD band was excised and sent to Harvard Microchem facility for sequencing by proteolytic digestion followed by mass spectrometry.

Acknowledgments

We wish to heartily thank Arshad Desai for providing tetrahymena axonemes as well as cheerful assistance with data analysis and encouragement, David King for performing mass spectometry on the 2X C18 fraction, Andrew Shiau for providing purified α-lytic protease, Josh Niclas for assistance with microscopy, and Jody Rosenblatt for introducing the lab to P.J. Harvey. We also thank Arshad Desai and Jody Rosenblatt for helpful comments on the manuscript. This work was supported by an NIH grant (GM 39565-07).

REFERENCES

Amin, H. S., and Wadsworth, P. (1991). Inhibition of spindle elongation by taxol. Cell Motil Cytoskeleton *20*, 136-44.

Andersen, S. S., Buendia, B., Dominguez, J. E., Sawyer, A., and Karsenti, E. (1994). Effect on microtubule dynamics of XMAP230, a microtubule-associated protein present in Xenopus laevis eggs and dividing cells. J Cell Biol *127*, 1289-99.

Belmont, L. D., Hyman, A. A., Sawin, K. E., and Mitchison, T. J. (1990). Real-time visualization of cell cycle-dependent changes in microtubule dynamics in cytoplasmic extracts. Cell *62*, 579-89.

Beretta, L., Dobransky, T., and Sobel, A. (1993). Multiple phosphorylation of stathmin. Identification of four sites phosphorylated in intact cells and in vitro by cyclic AMP-dependent protein kinase and p34cdc2. J Biol Chem *268*, 20076-84.

Braverman, R., Bhattacharya, B., Feuerstein, N., and Cooper, H. L. (1986). Identification and characterization of the nonphosphorylated precursor of pp17, a phosphoprotein associated with phorbol ester induction of growth arrest and monocytic differentiation in HL-60 promyelocytic leukemia cells. J Biol Chem *261*, 14342-8.

Cassimeris, L., Pryer, N. K., and Salmon, E. D. (1988). Real-time observations of microtubule dynamic instability in living cells. J Cell Biol *107*, 2223-31.

Correia, J. J. (1991). Effects of Antimitotic Agents on Tubulin-Nucleotide Interactions. Pharmac. Ther. *52*, 127-47.

Curmi, P. A., Maucuer, A., Asselin, S., Lecourtois, M., Chaffotte, A., Schmitter, J. M., and Sobel, A. (1994). Molecular characterization of human stathmin expressed in Escherichia coli: site-directed mutagenesis of two phosphorylatable serines (Ser-25 and Ser-63). Biochem J *300*, 331-8.

Drechsel, D. N., Hyman, A. A., Cobb, M. H., and Kirschner, M. W. (1992). Modulation of the dynamic instability of tubulin assembly by the microtubule-associated protein tau. Mol Biol Cell *3*, 1141-54.

Gliksman, N. R., Parsons, S. F., and Salmon, E. D. (1992). Okadaic acid induces interphase to mitotic-like microtubule dynamic instability by inactivating rescue. J Cell Biol *119*, 1271-6.

Gliksman, N. R., Skibbens, R. V., and Salmon, E. D. (1993). How the transition frequencies of microtubule dynamic instability (nucleation, catastrophe, and rescue) regulate microtubule dynamics in interphase and mitosis: analysis using a Monte Carlo computer simulation. Mol Biol Cell *4*, 1035-50.

Gotoh, Y., Nishida, E., Matsuda, S., Shiina, N., Kosako, H., Shiokawa, K., Akiyama, T., Ohta, K., and Sakai, H. (1991). In vitro effects on microtubule

dynamics of purified Xenopus M phase-activated MAP kinase. Nature *349*, 251-4.

Hanash, S. M., Strahler, J. R., Kuick, R., Chu, E. H., and Nichols, D. (1988). Identification of a polypeptide associated with the malignant phenotype in acute leukemia. J Biol Chem *263*, 12813-5.

Hartwell, L. H., and Kastan, M. B. (1994). Cell cycle control and cancer. Science *266*, 1821-8.

Hirokawa, N. (1994). Microtubule organization and dynamics dependent on microtubule-associated proteins. Curr Opin Cell Biol *6*, 74-81.

Hotani, T. H. a. H. (1986). Visualization of the dynamic instability of individual microtubules dark-field microscopy. Nature *321*, 605-607.

Jordan, M. A., Thrower, D., and Wilson, L. (1992). Effects of vinblastine, podophyllotoxin and nocodazole on mitotic spindles. Implications for the role of microtubule dynamics in mitosis. J Cell Sci, 401-16.

Jordan, M. A., Toso, R. J., Thrower, D., and Wilson, L. (1993). Mechanism of mitotic block and inhibition of cell proliferation by taxol at low concentrations. Proc. Natl. Acad. Sci. *90*, 9552-56.

Larsson, N., Melander, H., Marklund, U., Osterman, O., and Gullberg, M. (1995). G2/M transition requires multisite phosphorylation of oncoprotein 18 by two distinct protein kinase systems. J Biol Chem *270*, 14175-83.

Luo, X. N., Mookerjee, B., Ferrari, A., Mistry, S., and Atweh, G. F. (1994). Regulation of phosphoprotein p18 in leukemic cells. Cell cycle regulated phosphorylation by p34cdc2 kinase. J Biol Chem *269*, 10312-8.

Marklund, U., Brattsand, G., Shingler, V., and Gullberg, M. (1993). Serine 25 of oncoprotein 18 is a major cytosolic target for the mitogen-activated protein kinase. J Biol Chem *268*, 15039-47.

Marklund, U., Osterman, O., Melander, H., Bergh, A., and Gullberg, M. (1994). The phenotype of a "Cdc2 kinase target site-deficient" mutant of oncoprotein 18 reveals a role of this protein in cell cycle control. J Biol Chem *269*, 30626-35.

Matsudaira, P. (1993). A Practical Guide to Protein and Peptide Purification for Microsequencing, 2nd Edition, P. Matsudaira, Academic Press, INC.

Mitchison, T., and Kirschner, M. (1984). Dynamic instability of microtubule growth. Nature *312*, 237-42.

Murray, A. (1994). Cell cycle checkpoints. Curr Opin Cell Biol *6*, 872-6.

Ookata, K., Hisanaga, S., Bulinski, J. C., Murofushi, H., Aizawa, H., Itoh, T. J., Hotani, H., Okumura, E., Tachibana, K., and Kishimoto, T. (1995). Cyclin B interaction with microtubule-associated protein 4 (MAP4) targets p34cdc2 kinase to microtubules and is a potential regulator of M-phase microtubule dynamics. J Cell Biol *128*, 849-62.

Ookata, K., Hisanaga, S., Okumura, E., and Kishimoto, T. (1993). Association of p34cdc2/cyclin B complex with microtubules in starfish oocytes. J Cell Sci *105*, 873-81.

Pryer, N. K., Walker, R. A., Skeen, V. P., Bourns, B. D., Soboeiro, M. F., and Salmon, E. D. (1992). Brain microtubule-associated proteins modulate microtubule dynamic instability in vitro. Real-time observations using video microscopy. J Cell Sci *103*, 965-76.

Rowlands, D. C., Williams, A., Jones, N. A., Guest, S. S., Reynolds, G. M., Barber, P. C., and Brown, G. (1995). Stathmin expression is a feature of proliferating cells of most, if not all, cell lineages. Lab Invest *72*, 100-13.

Sackett, D. L. (1995). Vinca Site Agents Induce Structural Changes in Tubulin Differnt from and Antagonistic to Changes Induced by Colchicine Site Agents. Biochemistry *34*, 7010-19.

Salmon, E. D., Leslie, R. J., Karow, W. M., McIntosh, J. R., and Saxton, W. M. (1984). Spindle microtubule dynamics in sea urchin embryos. Analysis using fluorescence-labeled tubulin and measurements of fluorescence redistribution after laser photobleaching. J. Cell Biol. *99*, 2165-86.

Saxton, W. M., Stemple, D. L., Leslie, R. J., Salmon, E. D., Zavortink, M., and McIntosh, J. R. (1984). Tubulin dynamics in cultured mammalian cells. J. Cell Biol. *99*, 2175-86.

Schubart, U. K., Alago, W., Jr., and Danoff, A. (1987). Properties of p19, a novel cAMP-dependent protein kinase substrate protein purified from bovine brain. J Biol Chem *262*, 11871-7.

Shelden, E., and Wadsworth, P. (1993). Observation and quantification of individual microtubule behavior in vivo: microtubule dynamics are cell-type specific. J Cell Biol *120*, 935-45.

Shiina, N., Moriguchi, T., Ohta, K., Gotoh, Y., and Nishida, E. (1992). Regulation of a major microtubule-associated protein by MPF and MAP kinase. Embo J *11*, 3977-84.

Sobel, A. (1991). Stathmin: a relay phosphoprotein for multiple signal transduction? Trends Biochem Sci *16*, 301-5.

Sobel, A., Boutterin, M. C., Beretta, L., Chneiweiss, H., Doye, V., and Peyro-Saint-Paul, H. (1989). Intracellular substrates for extracellular signaling. Characterization of a ubiquitous, neuron-enriched phosphoprotein (stathmin). J Biol Chem *264*, 3765-72.

Toso, R. J., Jordan, M. A., Farrell, K. W., Matsumoto, B., and Wilson, L. (1993). Kinetic stabilization of microtubule dynamic instability in vitro by vinblastine. Biochemistry *32*, 1285-93.

Vandre, D. D., Centonze, V. E., Peloquin, J., Tombes, R. M., and Borisy, G. G. (1991). Proteins of the mammalian mitotic spindle:

phosphorylation/dephosphorylation of MAP-4 during mitosis. J Cell Sci *98*, 577-88.

Verde, F., Dogterom, M., Stelzer, E., Karsenti, E., and Leibler, S. (1992). Control of microtubule dynamics and length by cyclin A- and cyclin B-dependent kinases in Xenopus egg extracts. J Cell Biol *118*, 1097-108.

Verlhac, M. H., Kubiak, J. Z., Clarke, H. J., and Maro, B. (1994). Microtubule and chromatin behavior follow MAP kinase activity but not MPF activity during meiosis in mouse oocytes. Development *120*, 1017-2.

Wadsworth, P., and Salmon, E. D. (1986). Microtubule dynamics in mitotic spindles of living cells. Ann N Y Acad Sci *466*, 580-92.

Walker, R. A., O'Brien, E. T., Pryer, N. K., Soboeiro, M. F., Voter, W. A., Erickson, H. P., and Salmon, E. D. (1988). Dynamic instability of individual microtubules analyzed by video light microscopy: rate constants and transition frequencies. J Cell Biol *107*, 1437-48.

Figure Legends

Figure 1 Rapid Microtubule Inhibition Assay

A) Rhodamine tubulin assembly assay with a buffer control. B) Rhodamine tubulin assembly with a partially purified active fraction at 4 U/μl. Note the background fluorescence is higher when the rhodamine tubulin is not in polymer or large aggregates. The bar is 10 μM.

Figure 2 Purification of the MT Destabilizing Activity

An SDS polyacrylamide gel of (a) High speed supernatant (HSS), (b) boiled HSS, (c) MeOH precipitate, (d) first C18 peak, (e) second C18 peak. Lane (e) is the 2X C18 fraction used in all subsequent characterization of activity.

Figure 3 The MT Destabilizing Activity is Protease Sensitive

a) 2X C18 fraction b) 2X C18 fraction after incubation with 0.7μg of α-lytic protease, c) 0.7μg of α-lytic protease, d) 2X C18 fraction mixed with 0.7μg of α-lytic protease pre-incubated with an inhibitor. The presence of MTs in the MT assembly assay is designated by a +. The presence of MTs means there is no inhibition of MT assembly.

Figure 4 The Peak of Activity Coincides with the Peak of the 17.2 kD Protein

A) The fractions around the peak of activity from the C18 column were analyzed by SDS PAGE. The fractions marked with + or +/- had MT destabilizing activity and were pooled and run over a sizing column. B) Fractions collected from the sizing column. Fraction 3 had measurable MT destabilizing activity (1 U/μl), and fractions 2, 4 and 5 had activity after concentration. No other fractions had MT destabilizing activity. C) We

scanned the gel in 3B and measured the band intensity of the four visible bands. The dotted line shows the relative activity in each fraction, and the relative intensity of the four bands are shown with solid lines, 40 kD (▲), 17.2 kD (◆), 16 kD(□), 12.6 kD (●). The 17.2 kD band is the only protein whose band intensity has the same profile as the activity profile.

Figure 5 The 17.2 kD Protein Binds Unpolymerized Tubulin Dimers
A) Purified tubulin in the absence of GTP was mixed with an equimolar amount of the 2X C18 fraction, incubated at 37°C for 10' and fractionated on a sizing column. The 17.2 kD band normally elutes in fractions 7 and 8, but elutes entirely with the tubulin when they are mixed. The tubulin elution time is not appreciably different. B) The 2X C18 fraction was mixed with taxol MTs, incubated at 37°C for 10', and the MTs were sedimented through a glycerol cushion to separate MTs from unpolymerized. S designates the supernatant and P designates the pellet. (a) 2X C18 fraction was added after stabilization of MTs with taxol, (b) 2X C18 fraction was added prior to taxol addition, (c) 2X C18 fraction with taxol, d) tubulin with taxol. The 17.2 kD protein is almost entirely in the supernatant and only a small amount pellets with the MTs, about the same amount that pellets in the absence of MTs (lane c). When the 2XC18 fraction is added prior to the taxol it inhibits the stabilization of MTs by taxol.

Table Legends

Table 1 Purification Table

The starting material was 50 mls of high speed supernatant of fetal calf thymus. A unit of activity per μl is defined as the fold dilution at which more than 50% inhibition of MT assembly is still observed in the rhodamine tubulin assembly assay.

Table 2 Effects on Dynamic Parameters of Microtubules

The 2X C18 fraction (8U/μl) was diluted 10 fold into the given concentrations of tubulin and mixed with 2mM GTP and sea urchin axonemes. This mixture was flowed into a chamber, warmed to 35.5°C, observed with video-enhanced DIC microscopy and recorded for 10' to 15'. MT dynamic parameters were calculated for nine to twenty MTs for each condition, for a total observation time of approximately 2400 sec per condition. The +/- indicates the standard deviation.

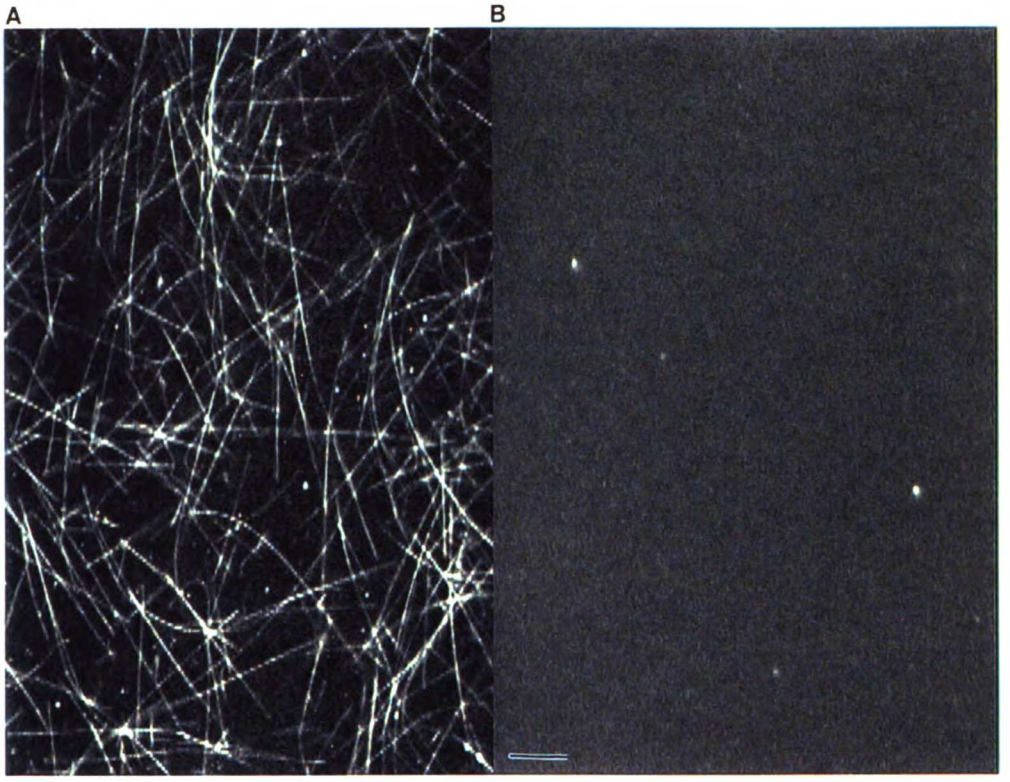
A
B

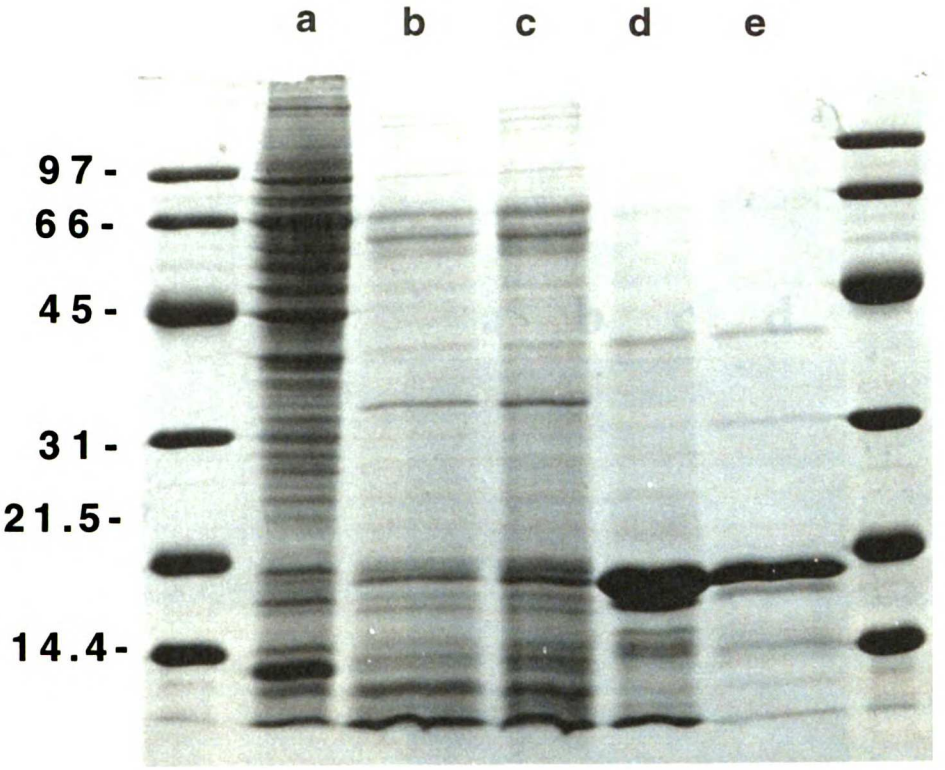
a
b
c
d
e
97-
66-
45-
31-
21.5-
14.4-

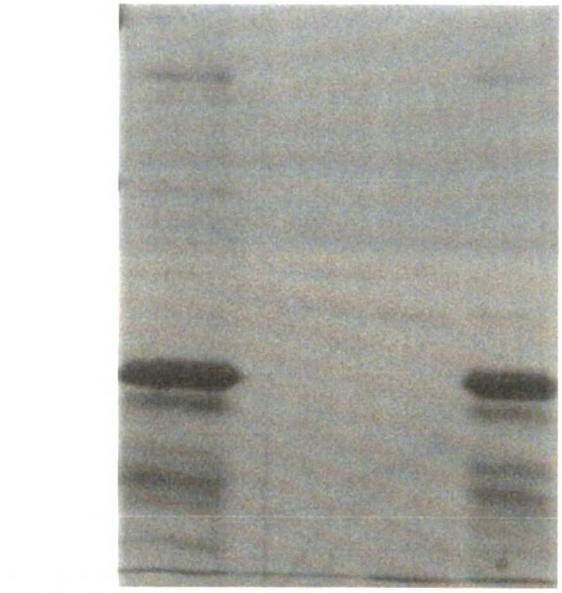
a b c d
MTs - + + -

A

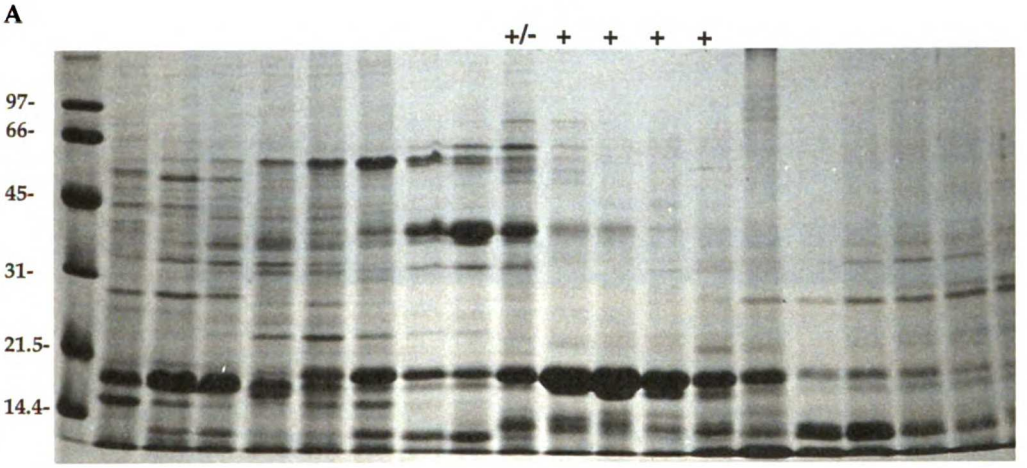
+/- + + + +
97-
66-
45-
31-
21.5-
14.4-

B

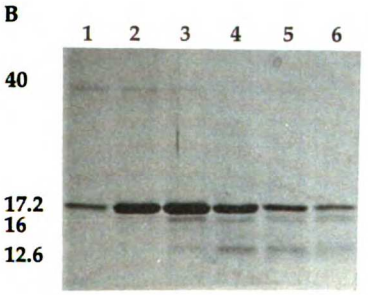
1 2 3 4 5 6
40
17.2
16
12.6

C

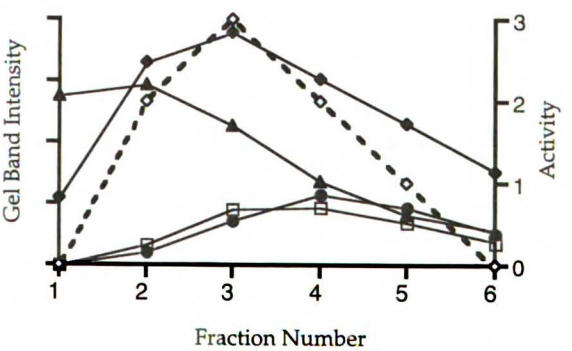
Gel Band Intensity
Activity
0
1
2
3
1 2 3 4 5 6
Fraction Number

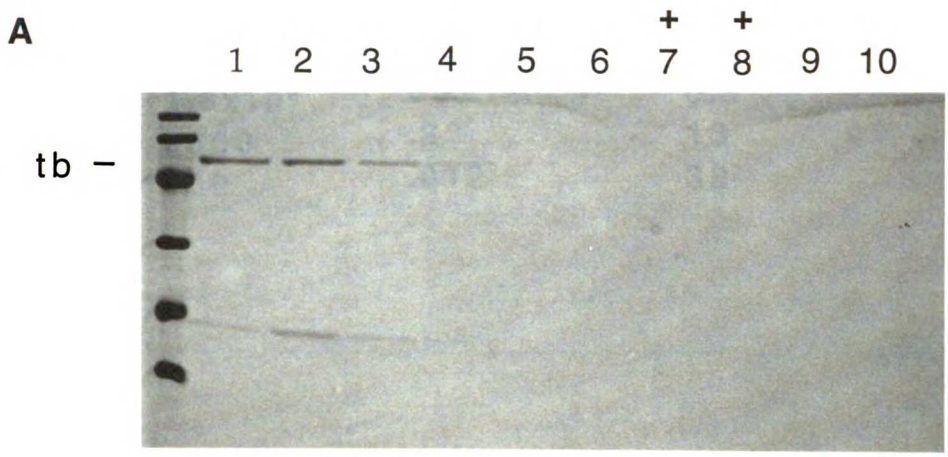
A
1 2 3 4 5 6 7 8 9 10
+ +
tb –

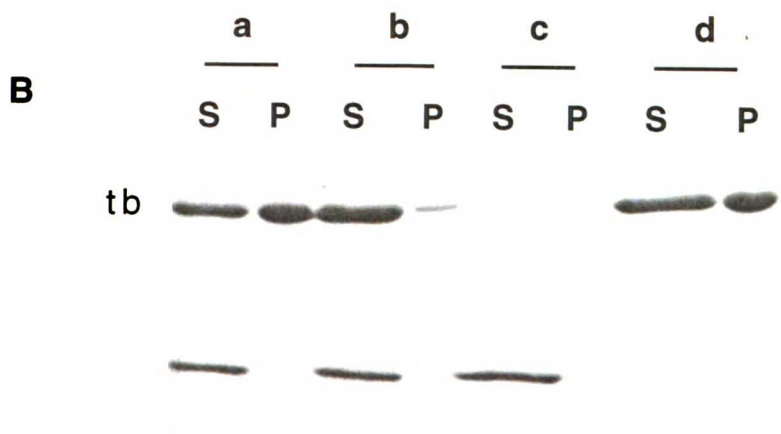
B
a b c d
S P S P S P S P
tb

PURIFICATION TABLE

Fraction	Activity	Protein(mg)	Specific Activity (U/μg)	% Total
HSS	1.1×10^5	1320	0.08	100
Boiled HSS	6.8×10^4	63	1.1	61
MeOH ppt	1.8×10^4	63	0.3	16
C18 Peak	2600	.2	13	2.4
Sizing Peak	400	.012	33	0.4

Tubulin (μM)	Growth Rate (μm/s)		Catastrophe Frequency (s^{-1}) x10 $^{-4}$	
	tb +buffer	tb +AF	tb +buffer	tb +AF
15	0.022 +/-0.005	0.013+/-0.005	8.4	66
18	0.029+/-0.013	0.020+/-0.01	4.6	47
20	0.035+/-0.017	0.021+/-0.007	5.6	26

Chapter 3

A Cellular Factor that Increases the Catastrophe Frequency of Microtubules and Destabilizes GMPCPP Microtubules.

Abstract

We have partially purified a factor from calf thymus and *Xenopus* eggs that increases the catastrophe frequency of microtubules. Analysis of dynamic parameters suggests that this factor acts by increasing the off rate of GTP tubulin. This model is further supported by experiments demonstrating that the factor destabilizes microtubules polymerized with the slowly hydrolyzable GTP analog, GMPCPP, without increasing the rate of hydrolysis of this analog.

Introduction

Microtubule (MT) polymers interconvert between phases of slow growth and rapid shortening, with abrupt transitions between the two phases (Mitchison and Kirschner, 1984). Transitions from growing to shrinking are called catastrophes and transitions from shrinking to growing are called rescues. Growth and shrinkage is due to addition or loss of tubulin subunits from the ends of MTs, respectively. MTs assemble from tubulin bound to GTP, and the hydrolysis of this GTP is necessary for disassembly. Therefore, growth is assumed to result from addition of GTP tubulin, and shrinkage primarily results from loss of GDP tubulin. This behavior, termed dynamic instability, has been observed *in vitro* (Hotani, 1986; Walker et al., 1988), in cellular extracts (Belmont et al., 1990; Gliksman et al., 1992), and *in vivo* in many cell types (Cassimeris et al., 1988; Shelden and Wadsworth, 1993). Microtubules have an intrinsic polarity and are more dynamic on their faster growing plus ends; *in vivo*, most minus ends are

anchored to MTOCs, while plus ends grow and shrink. Proper control of MT dynamics is essential for many MT dependent processes, including mitotic spindle assembly and function and a detailed understanding of the mechanism of dynamic instability may eventually lend insights into these important processes.

Walker et al (1988) carried out extensive analysis of MTs undergoing dynamic instability. By using video microscopy to analyze MTs, they were able to make independent observations of growing MTs within a population in which MTs were growing and shrinking. One interesting result from these studies was that when the growth rate determined from the population of growing MTs was plotted against the tubulin concentration, the y-intercept was negative. Assuming that all tubulin subunits at the plus end of a growing MT are bound to GTP this suggests that there is a measurable off rate of GTP tubulin.

Bayley et al (1990) have proposed the lateral cap model to account for dynamic instability behavior of MTs. In this model they propose that hydrolysis of GTP is coupled to subunit addition, resulting in a single layer GTP tubulin cap. The frequency of transitions is determined by the off rates of tubulin subunits on the end of a microtubule, and these rates are determined by the nucleotide bound to the subunit and to the neighboring subunits. One prediction of this model is that increasing the off rate of GTP tubulin with neighboring GTP tubulin subunits will increase the catastrophe frequency. Hyman et al (1992) have demonstrated that the GTP analog, GMPCPP, stabilizes MTs and is hydrolyzed very slowly by MTs. We have found this analog to useful in dissecting the mechanism of dynamic instability as well as regulators of MT dynamics. In this work we have looked for cellular regulators that increase the catastrophe frequency of MTs.

We present evidence that a small molecular weight factor increases the catastrophe frequency of MTs and destabilizes MTs polymerized with GMPCPP.

Methods

Purification

The active fraction was partially purified from frog eggs and calf thymus using a rapid rhodamine tubulin assay (Belmont et al., 1995). Extracts of Xenopus eggs arrested in metaphase of meiosis II, and thymus extracts were prepared as described were prepared as described (Belmont et al., 1990, 1995). A high speed supernatant (HSS) was prepared by spinning a crude extract in a TLA100.3 rotor for 1 hr at 100,000 rpm. 2-ME was added to 1% to the supernatant, this was boiled for 15', and the denatured protein was sedimented in an eppendorf microfuge or an SS34 for 10' at top speed at 4°C. A 50-65% ammonium sulfate precipitate from the boiled HSS was collected and loaded onto a GlasPac TSK G3000SW (LKB 2135-830) sizing column equilibrated with AB (80 M K Pipes pH 7.5, 5mM $MgCl_2$, 1mM EGTA) and run at 0.3 ml/min. The peak of activity from this column is the active fraction characterized below. Protein concentrations were estimated using Bradford reagent.

Real Time Microscopy

7 μl of a peak from the sizing column was mixed with 1 μl of sea urchin axonemes and 2 μl tubulin and GTP. The final concentration of GTP was 2 mM and the final concentration of tubulin ranged from 7 to 28 μM. The stage was heated to 37°C with a heater. MTs were observed by video enhanced DIC (VEDIC), images were recorded as described (Belmont and Mitchison, 1995), and measurements were performed with a ruler on a large screen monitor. Between 10 and 20 microtubules were measured for each condition. Growth rates were determined by dividing the change in length by the time between 2 points at which the plus end was clearly resolved. Catastrophe frequencies were calculated as the number of catastrophes observed divided by the total observed growth time of all growing MTs.

GMPCPP Microtubules

Rhodamine labeled GMPCPP (guanylyl-(a,b)-methylene-diphosphonate) microtubules were made by mixing 0.4 mg/ml tubulin (3:1 unlabeled:labeled) with 0.18 mM GMPCPP and incubating at 37°C for 1 hour. These microtubules were diluted 20 fold into either AB, nocodazole (10 μg/ml) or the active fraction from the sizing column. At various time points, 4 μl of this mixture was added to 40 μl of 0.5% glutaraldehyde, and 20 μl of this was diluted into 1 ml of BRB80. The MTs were sedimented onto 12mm coverslips at 12,000 rpm for 1 hr in a swinging bucket rotor. The number of microtubules per field was counted for 20 fields per condition. For experiments measuring the depolymerization rate, the microtubules were diluted an additional 10 fold and polymerized for an additional hour to

produce longer microtubules. The length of approximately 150 microtubules were measured for each time point.

$\gamma^{32}P$ labeled GMPCPP was made by mixing 5 µl of $\gamma^{32}P$ ATP (3000 Ci/mmol, 10 mCi/ml), 1µl 10X NDPK buffer (0.2M Tris pH 8.0, 0.5 M NaCl, 0.05 M $MgCl_2$, 1% 2-ME), 1.5 µl GMPCP (1mM), 0.5 µl nucleotide diphosphate kinase (NDPK, 1000U/ml), and 2 µl water. This was incubated for 4 hrs at 25°C. GMPCPP was added to a final concentration of 0.5 mM, the mix was spun through a Millipore filter with a 10 kD cutoff, and the follow-through was collected. The final product was confirmed by spotting 2.5 µl onto PEI TLC plates and analyzed as described (Hyman et al., 1992).

To measure the effect of the active fraction on hydrolysis of GMPCPP in MTs we mixed 4 µl of 35 mg/ml tubulin (4:1 unlabeled:rhodamine labeled), 2.8 µl $\gamma^{32}P$ labeled GMPCPP (0.5 mM) with 3.2 µl of AB. The final concentrations were 140µM tubulin, 140 µM GMPCPP. This was polymerized at 37°C for 1.5 hr, layered onto a 160 µl cushion of warm 60% glycerol in AB and spun at 100,000 rpm for 5' at 35°C. The pellet was washed with 160 µl warm AB and resuspended in 10 µl of warm AB. 4 µl of these MTs were mixed with 36 µl of either warm AB or active sizing column fraction. At various time points, 3µl of this mixture was added to 6 µl of formaldehyde and frozen in liquid nitrogen. These were spotted onto TLC plates and the quantified on a phospho-imager.

Size Determination

The size of the active fraction was measured on a Supelco G3000PWXL sizing column equilibrated with AB and run at 0.3 ml/min. We used a peptide mix (Sigma) with peptides of 1046, 573, 555, and 415 Da, as well as

profilin (15,000 Da) and human chorionic gonadotropin (HCG, 3876 Da) for size standards. The MW was estimated by plotting the log of the MW versus the retention time.

Results

Purification

A destabilizing activity was identified using an assay designed to identify inhibitors of MT assembly. In this assay we add rhodamine tubulin, GTP, and axonemes to extract fractions and look for fractions that cause a decrease in the number or length of MTs nucleated from axonemes. A destabilizing activity was found in a 50 to 65% ammonium sulfate cut of a boiled high speed supernatant of both *Xenopus* egg and calf thymus extracts. This activity was further purified on a sizing column. The resultant fraction contained very few proteins by silver stain. The only bands consistently observed were at 4 and 8 kD by PAGE on an 18% gel. The activity was not sensitive to trypsin, pronase E, or RNAse A. The size was later determined on a higher resolution column. There were two peaks of activity from calf thymus, at 1700 Da and 2600 Da, and one peak of activity from *Xenopus* egg extracts at 1700 Da. These activities are distinct from the 17,220 Da protein characterized previously (Belmont and Mitchison, 1995). Estimates of protein concentration during purification are shown in table 1.

Videomicroscopy Analysis

Parameters of dynamic instability were measured using video-enhanced differential interference contrast (VEDIC) microscopy. Tubulin and GTP were added to active fractions from the sizing column and MTs were recorded undergoing dynamic instability in real time. Growth rates and catastrophe frequencies at various tubulin concentrations with and without the active fraction are shown in table 2. These data show a decrease in the growth rate and an increase in catastrophe frequency in the presence of the active fraction. The three simplest explanations for this observation are i) a decrease in the on rate of GTP tubulin, ii) an increase in the off rate of GTP tubulin, or iii) a decrease in the effective tubulin concentration. The on rate of GTP tubulin is determined by the slope of the line of growth rate vs. tubulin concentration. Therefore, a decrease in the on rate of GTP tubulin would result in a decrease in the slope of this line. The off rate of GTP tubulin is the y-intercept of this line (Walker et al., 1988), so an increase in the off rate should result in a decrease in the y-intercept. A decrease in the effective tubulin concentration should result in no change in the slope of this line and an increase in the x-intercept (and decrease in the y-intercept). See figure 1 for a graphical representation of this.

To distinguish between these possibilities, we plotted the growth rate as a function of tubulin concentration (figure 2a). There was only a slight decrease in the slope and a large decrease in the y intercept. This suggested that the observed changes in MT dynamics were unlikely to be due to a decrease in the on rate of GTP tubulin. To distinguish between the other to models we plotted catastrophe frequency as a function of growth rate. If the observed changes were due simply to a decrease in the effective tubulin concentration, there should be no change in the catastrophe frequency at a given growth rate. However, figure 2b shows that there is an increase in the

catastrophe frequency plotted as a function of growth rate. This suggests that the observed changes in dynamic instability are not simply due to decreasing the amount of tubulin available for assembly, and may be due to an increase in the off rate of GTP tubulin on growing microtubules. An alternative explanation is that there is an increase in the rate of GTP hydrolysis on the polymer. This will be addressed in the next section.

The Activity Increases the Depolymerization Rate of GMPCPP MTs

To further characterize the activity, we tested its ability to destabilize microtubules polymerized with a very slowly hydrolyzable GTP analog, GMPCPP. Microtubules polymerized with this analog are stable for many days at room temperature (Hyman et al., 1992) in BRB80, but are depolymerized in less that 10 minutes in a crude *Xenopus* extract (data not shown). Figure 3a shows that rhodamine tubulin GMPCPP MTs are gone in a matter of hours in the presence of the active fraction. By measuring length as a function of time in the presence of the active fraction, we determined that this due to an increase in the rate of depolymerization of GMPCPP MTs (figure 3b). The off rate determined for GMPCPP tubulin in the presence of the factor was 0.43 dimers/sec (assuming 1634 dimers/μm). The off rate was 0.08 s^{-1} in buffer, and 0.23 s^{-1} in 10μg/ml nocodazole. The active fraction increases the off rate of GMPCPP tubulin by 5 fold over buffer, and nearly 2 fold over nocodazole.

The Activity Does Not Increase the Rate of Hydrolysis of GMPCPP

We next wanted to determine if the destabilization of GMPCPP microtubules was due to an increase in the rate of hydrolysis of this analog in the presence of the active fraction. We labeled the γ phosphate of GMPCPP with ^{32}P, and made rhodamine tubulin GMPCPP* microtubules. These were incubated in the presence or absence of the active fraction and aliquots were examined on TLC at various time points. Figure 4a shows that the initial rate of hydrolysis of GMPCPP is not increased in the presence of the active fraction. The rate of hydrolysis of this GTP analog in MTs in the presence of the active fraction is nearly zero after 4 hrs, the time at which all the microtubules are gone. Therefore, we conclude that the destabilization of GMPCPP microtubules is not due to an increase in the rate of hydrolysis of GMPCPP in the presence of the activity, and probably results from an increase in the off rate of GMPCPP-tubulin from MT ends.

Discussion

In this work we partially purified a small molecular weight factor that increases the catastrophe frequency and decreases the growth rate of microtubules. The increase in catastrophe frequency is more than would be expected simply from decreasing the growth rate, suggesting that it specifically affects the catastrophe frequency. Analysis of dynamic parameters of MTs suggest that it may act by increasing the off rate of GTP tubulin from the ends of growing microtubules. This model is further supported by experiments demonstrating that the activity increases the off rate of GMPCPP-tubulin, without increasing the rate of hydrolysis. This GTP analog is very slowly hydrolyzed on MTs, and hydrolysis of GTP is necessary

for depolymerization of pure tubulin. The active fraction seems to circumvent the requirement for nucleotide hydrolysis for depolymerization.

Current models predict that dynamic instability can be modulated by the off rate of GTP bound tubulin and predict that increasing this rate will increase the catastrophe frequency (Bayley et al., 1990). The results presented here suggest that there may be a cellular factor that regulates MT transition frequencies by increasing this rate. This is consistent with earlier studies showing that transition frequencies are a major regulated dynamic parameter of MTs (Belmont et al., 1990; Gliksman et al., 1992; Shelden and Wadsworth, 1993).

References

Bayley, P. M., Schilstra, M. J., and Martin, S. R. (1990). Microtubule dynamic instability: numerical simulation of microtubule transition properties using a Lateral Cap model. J Cell Sci, 33-48.

Belmont, L. D., Hyman, A. A., Sawin, K. E., and Mitchison, T. J. (1990). Real-time visualization of cell cycle-dependent changes in microtubule dynamics in cytoplasmic extracts. Cell *62*, 579-89.

Belmont, L.D., and Mitchison, T.J. (1995). The identification of a protein that increases the catastrophe frequency of microtubules and binds tubulin dimers. submitted

Cassimeris, L., Pryer, N. K., and Salmon, E. D. (1988). Real-time observations of microtubule dynamic instability in living cells. J Cell Biol *107*, 2223-31.

Gliksman, N. R., Parsons, S. F., and Salmon, E. D. (1992). Okadaic acid induces interphase to mitotic-like microtubule dynamic instability by inactivating rescue. J Cell Biol *119*, 1271-6.

Hotani, T. H. a. H. (1986). Visualization of the dynamic instability of individual microtubules dark-field microscopy. Nature *321*, 605-607.

Hyman, A. A., Salser, S., Drechsel, D. N., Unwin, N., and Mitchison, T. J. (1992). Role of GTP hydrolysis in microtubule dynamics: information from a slowly hydrolyzable analogue, GMPCPP. Mol Biol Cell *3*, 1155-67.

Mitchison, T., and Kirschner, M. (1984). Dynamic instability of microtubule growth. Nature *312*, 237-42.

Shelden, E., and Wadsworth, P. (1993). Observation and quantification of individual microtubule behavior in vivo: microtubule dynamics are cell-type specific. J Cell Biol *120*, 935-45.

Walker, R. A., O'Brien, E. T., Pryer, N. K., Soboeiro, M. F., Voter, W. A., Erickson, H. P., and Salmon, E. D. (1988). Dynamic instability of individual microtubules analyzed by video light microscopy: rate constants and transition frequencies. J Cell Biol *107*, 1437-48.

Figure Legends

Table 1 Partial Purification of a MT Destabilizing Factor

The active fraction was partially purified using an assay that identifies MT destabilizing activities. Protein concentrations of active fractions were determined by Bradford assays.

Table 2 Parameters of Dynamic Instability

MTs were observed undergoing dynamic instability by VEDIC at 37°C. 7μl of the sizing column fraction was added to 3 μl of tubulin, GTP and axonemes and the growth rates and catastrophe frequencies were measured on plus ends of MTs. Slides were observed for a maximum time of 15 minutes.

Figure 1 Models for Observed Changes in Dynamic Instability

If the activity is simply making tubulin unavailable for assembly, we expect an increase in the x intercept of the growth rate vs. tubulin concentration. If the activity causes a decrease in the on rate of tubulin, we expect a decrease in the slope, and if the activity increases the off rate of GTP tubulin, we expect a decrease in the y intercept of this line.

Figure 2 Observed Effects on Dynamic Instability

A. Growth rates of plus ends are shown as a function of tubulin concentration for tubulin plus buffer (o), the active fraction from frog (□), and the active fraction from calf thymus (◇) The primary change is a decrease in the y intercept, with only small changes in the slope. The equations derived from a linear regression are: buffer, y=-0.001 +0.0034x (R=0.98); frog fraction, y=-0.01+0.0030x (R=0.98); thymus fraction, y=-

.008+0.0024x (R=0.97). B. The catastrophe frequency plotted as a function growth rates for tubulin plus buffer (o), the active fraction from frog (□), and the active fraction from calf thymus (◇). The increase in catastrophe in the presence of the activity is greater than expected simply from lowering the growth rate.

Figure 3 Destabilization of GMPCPP MTs

A. The number of GMPCPP MTs per field was counted in the presence of buffer (o) and the active fraction from calf thymus (□). Twenty fields were counted for each time point. B The length of MTs in buffer (o) or the active fraction from calf thymus (□) was measured for 150 to 200 MTs per time point for each condition. The slope of the line in the buffer control is -0.18 and the slope in the presence of the active fraction is -0.95. The gives an off rate of GMPCPP tubulin of 0.08 s^{-1} in buffer and 0.43 s^{-1} in the presence of the active fraction.

Figure 4 Hydrolysis of GMPCPP by MTs

We measure the hydrolysis of GMPCPP in MTs in the absence (o) or presence (□) of the active fraction from calf thymus. In the first 4 hours (A) the slopes of these two lines are identical (0.1). The MTs in the buffer control continue to hydrolyze GMPCPP over the next 66 hrs, but in the presence of the active fraction the rate of hydrolysis levels off after the MTs are gone.

Table 1

Fraction	Protein Concentration	Protein/ml crude extract
Crude Extract	80 mg/ml	80 mg
High Speed Sup	16 mg/ml	32 mg
Ammonium Sulfate, 50-65%	7.5 mg/ml	15 mg/ml
Boiled Ammonium Sulfate cut	1 mg/ml	0.2 mg
Sizing Column Peak	0.5μg/ml	0.5μg

Table 2

	Tubulin (μM)	n	Growth (μm/s)	sd	Cat Frequency (s^{-1})
Tubulin	7	15	0.025	0.008	0.0011
	14	15	0.041	0.01	0.0007
	21	12	0.072	0.023	<0.00098
Tb + Thymus Fraction	14	11	0.028	0.011	0.006
	21	10	0.038	0.015	0.0039
	28	6	0.062	0.02	0.003
Tb+Frog Fraction	10.5	11	0.023	0.016	0.012
	14	13	0.028	0.017	0.0065
	21	11	0.053	0.011	none

Figure 1

1. DECREASE EFFECTIVE TUBULIN CONCENTRATION
2. DECREASE ON RATE OF GTP TUBULIN
3. INCREASE OFF RATE OF GTP TUBULIN

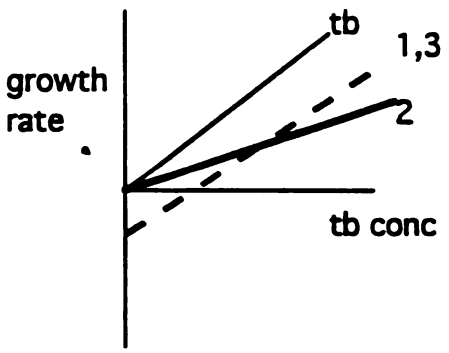

1. X INTERCEPT
2. SLOPE
3. Y INTERCEPT

Figure 2

A

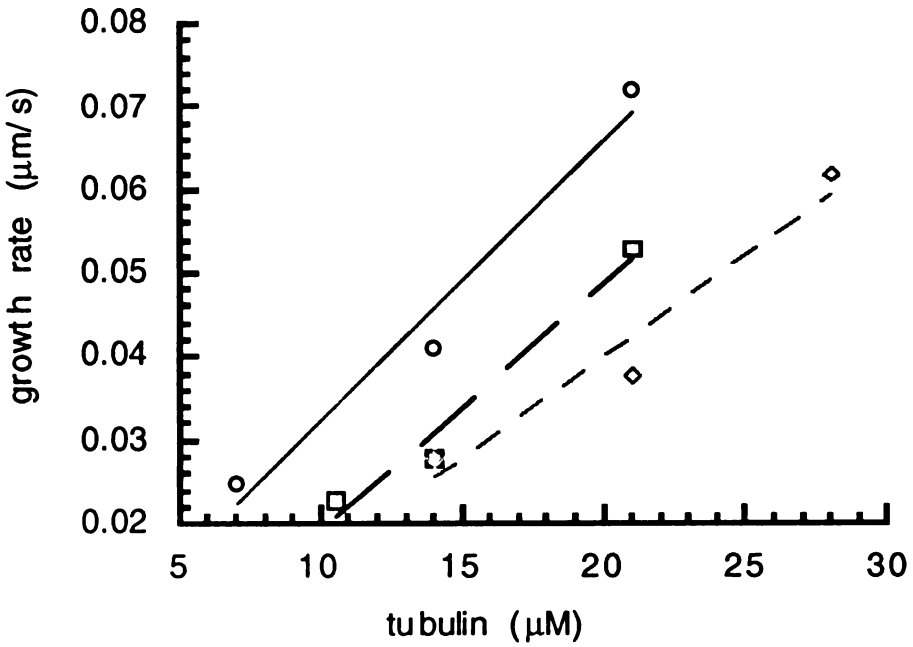
0.08
0.07
0.06
0.05
0.04
0.03
0.02
growth rate (µm/s)
5
10
15
20
25
30
tubulin (µM)

B

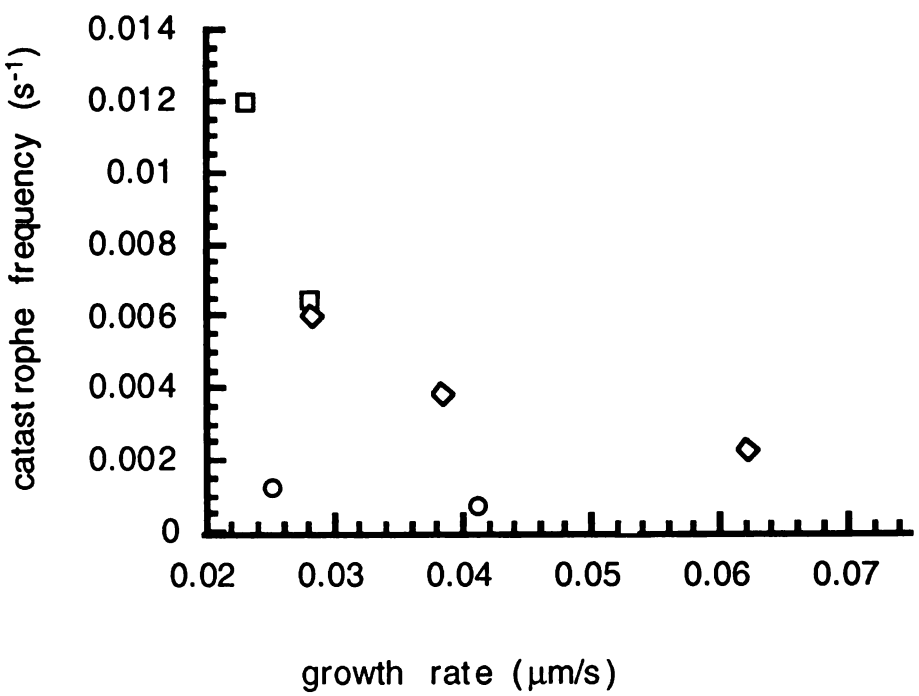
0.014
0.012
0.01
0.008
0.006
0.004
0.002
0
catastrophe frequency (s-1)
0.02
0.03
0.04
0.05
0.06
0.07
growth rate (µm/s)

Figure 3

A

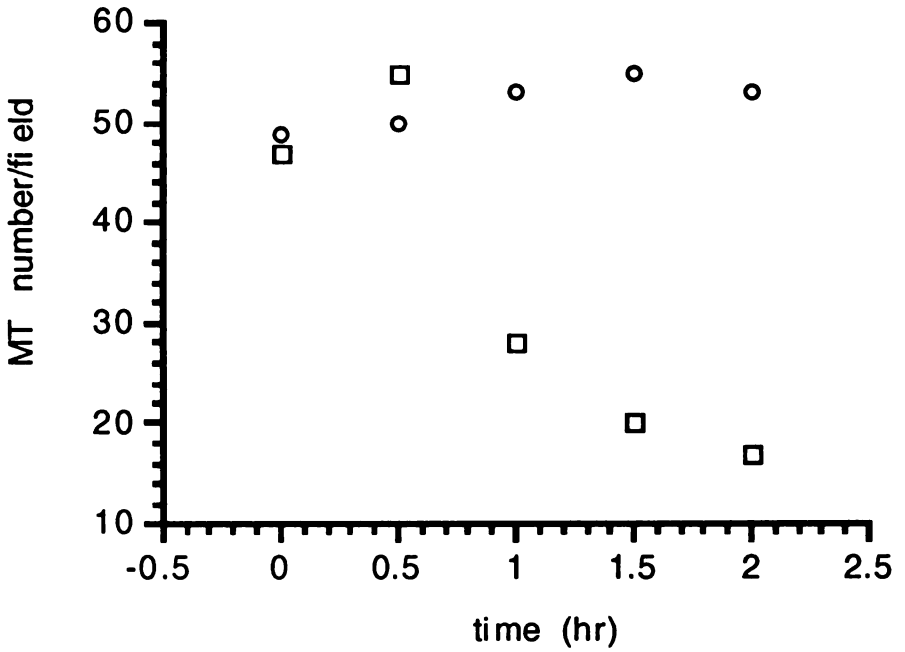
60
50
40
30
20
10
MT number/field
-0.5
0
0.5
1
1.5
2
2.5
time (hr)

B

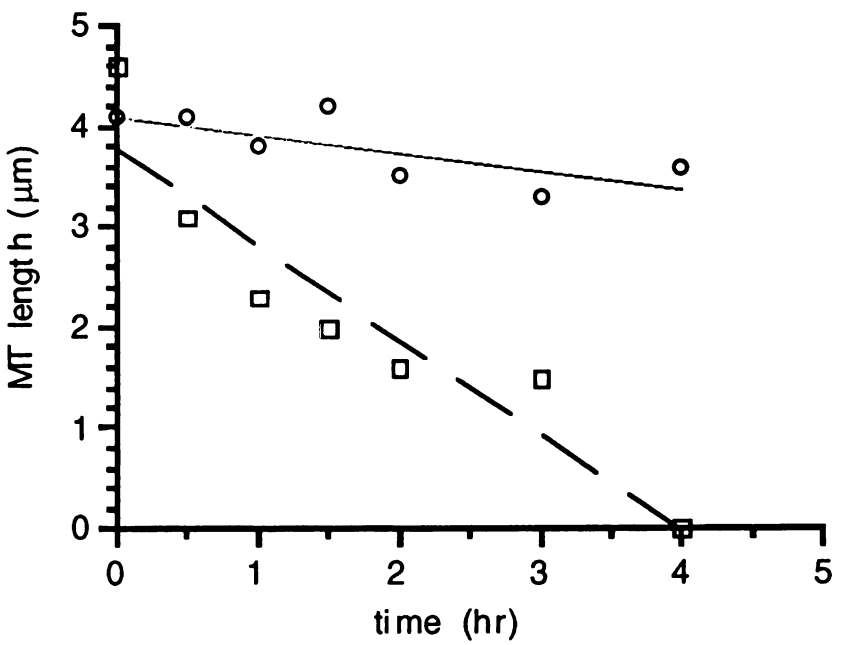
5
4
3
2
1
0
MT length (μm)
0
1
2
3
4
5
time (hr)

Figure 4

A

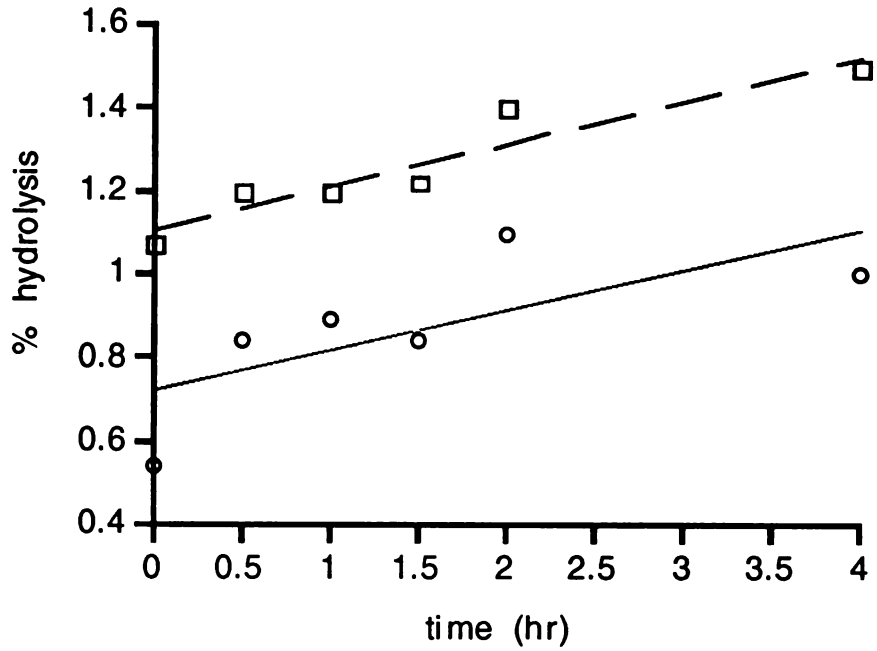
1.6
1.4
1.2
1
0.8
0.6
0.4
% hydrolysis
0
0.5
1
1.5
2
2.5
3
3.5
4
time (hr)

B

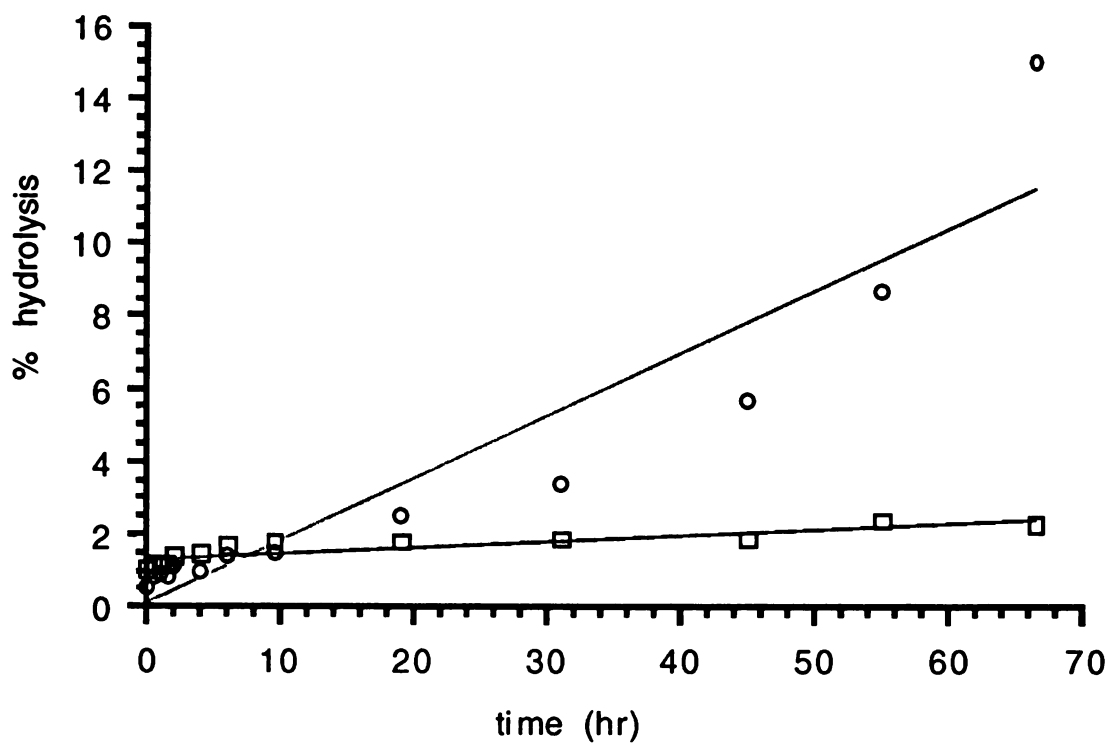
16
14
12
10
8
6
4
2
0
% hydrolysis
0
10
20
30
40
50
60
70
time (hr)

DISCUSSION

In conclusion, I will primarily discuss the implications of identifying Op18 as a catastrophe factor and future directions this project might take. However, I first want to say a few words about the other projects that didn't come to such a satisfying conclusion. I will discuss the tantalizing data on the very small molecular weight catastrophe factor as well as uses and limitations of the MT GTPase assay.

In the course of purifying Op18, I also partially purified a very small molecular weight factor that destabilized MTs. This factor was also heat stable and eluted from a sizing column at a position indicating a molecular weight of about 1700 Da. It could be partially purified by boiling a high speed supernatant of *Xenopus* or thymus extract and running the heat soluble fraction over a high resolution sizing column. By adding this partially purified factor to pure tubulin and analyzing MT dynamics with video-enhanced differential interference contrast (VEDIC) microscopy, I determined that it acted as a catastrophe factor. This fraction also showed a very impressive ability to destabilize GMPCPP MTs. We were unable to identify the factor responsible for this activity, largely due to inexperience in dealing with things that didn't behave as proteins or nucleic acids. The activity was not sensitive to the proteases tested, RNAse A, or NP40. I was unable to recover the activity from anion or cation exchange columns. However, this fraction showed very strong MT destabilizing activity and behaved functionally different from Op18 in its ability to destabilize GMPCPP stabilized MTs. Further characterization demonstrated that this factor stabilized GMPCPP MTs without increasing the rate of hydrolysis of this slowly hydrolyzable GTP analog. This, in conjunction with real time

analysis, suggested that it may act by increasing the off rate of GTP (or GMPCPP) tubulin. I would encourage anyone who was interested in trying to identify and further characterize this factor.

In any attempt to finish purifying this activity I would recommend the following. Omit the ammonium sulfate step and try would an organic extraction. I would test the solubility properties of the activity in solvents such as MeOH and EtOH. If it is soluble in these, try butanol, hexane and cyclohexane. After further purification, get the sample analyzed by mass spectometry to assess the purity.

The assay designed to measure GTPase activity on MT ends (appendix 2) has some use in characterizing purified components. However, this assay has serious limitations as an assay for identifying new factors. The main problem is that there are too many false positives. I thought I could escape this problem by measuring both MT and solution GTPase, and only selecting fractions that showed MT GTPase but no solution GTPase. The drawback with this solution is that essentially all fractions that elute from a sizing column in the normal molecular weight range for proteins either show solution and MT GTPase or no GTPase at all. If one wanted to pursue the identification of factors that increase the GTPase rate of MTs, I would recommend refining the assay until there are positives for MT GTPase that are clearly distinct from solution GTPases that are in the normal molecular weight range for proteins. However, I would not encourage anyone to pursue this project unless there is some evidence produced to support the existence of such factors.

Clearly the result of greatest interest is the identification of Op 18 as a MT catastrophe promoter. This protein was purified on the basis of its MT destabilizing activity, and shown to be a catastrophe factor by VEDIC analysis.

This protein also binds to unpolymerized tubulin dimers and inhibits stabilization of MTs by taxol when added prior to taxol. Studies from other labs suggest that Op18 may be regulated by phosphorylation in a cell cycle dependent manner. This information suggests numerous experiments. The first experiments, designed to look at the *in vivo* function of Op18 have already been initiated in our laboratory. Other labs have expressed antisense constructs to inhibit Op18 expression and seen a block at G2 and in M. It would be quite interesting to repeat those experiments and look carefully at MT staining patterns to determine if there a specific defect in MTs. Additionally, frog extracts provide an excellent experimental system in which to address questions of the role of Op18 in regulating MT dynamics and spindle assembly. We have made anti-peptide antibodies to *Xenopus* Op18 (stathmin) and immuno-precipitated this protein from mitotic extracts. This results in larger and brighter MT asters, as well as an increase in the number of free MTs. This indicates that the Op18 protein does have a role in destabilizing MTs in cellular extracts, and most likely *in vivo*. More careful studies to dissect the role of this protein in MT dynamics and spindle assembly and function are in progress.

There are also a number of experiments that will address mechanistic questions of Op18 function. The first obvious experiment is to dissect the functional importance of Op18 phosphorylation. A number of careful studies have yielded a map of the phosphorylation sites on Op18 and demonstrated that these sites can be phosphorylated *in vitro* on bacterially expressed or purified Op18. Therefore, we have the tools in hand to determine how phosphorylation on these sites influences the ability of Op18 to bind to tubulin dimers and to destabilize MTs. This should provide mechanistic insights into Op18 functions *in vivo*, specifically can

phosphorylation change its affinity for tubulin or its ability to de-stabilize MTs? It is also possible that phosphorylation of Op18 changes its affinity for other proteins. This question can be addressed by expressing Op18 constructs with mutated phosphorylation sites and immunoprecipitating the resulting proteins from extracts or cells, or immuno-precipitating endogenous Op18 at various stages in the cell cycle.

A very interesting and testable hypothesis is that Op18 could modulate the nucleotide bound to the tubulin dimer. This type of regulation is seen with actin binding proteins, but has never been reported for tubulin. Vandecandelaere et al., (1995) have demonstrated that increasing the ratio of GDP to GTP tubulin can in fact increase the frequency of catastrophes with little effect on growth rates. It will be straightforward to test the affinity of Op18 for GTP and GDP tubulin using the gel filtration assay described in chapter 2. Op18 could increase the ratio of GDP to GTP tubulin simply by having a higher affinity for GDP tubulin. At present, Op18 (with an undefined phosphorylation state) has only been tested for its ability to bind GDP tubulin.

Another potential study is to determine if Op18 could be used to assist in the crystallization of tubulin. It has been difficult to crystallize cytoskeletal polymer subunits because they tend to polymerize under crystal forming conditions. This problem was overcome for actin by co-crystallizing with DNase I, a protein with a high affinity for actin. It is possible that Op18 could be used in a similar way to crystallize tubulin. Preliminary results from the sizing column indicate that there may be two Op18 binding sites on a tubulin dimer. Even if Op18 does not facilitate the crystallization of tubulin, it may still be very interesting to know its crystal structure, for mechanistic information and for potential medical applications. Given the success of the

MT stabilizing drug, taxol, in cancer chemotherapy, inhibiting this destabilizer of MTs may also prove effective as a cancer therapy. Knowing the crystal structure may help in drug design.

I will conclude by proposing a general model incorporating the known regulators of MTs. MAPs, the best characterized regulators of MTs were discussed extensively in the introduction. Additionally, there are proteins that sever MTs (Shiina et al., 1992, McNally and Vale, 1993, Shiina et al., 1994), and recently a kinesin related protein, XKCM1 has also been shown to act as a catastrophe factor. Two MAPs found in dividing cells, MAP4 and XMAP230, are phosphorylated in mitosis and this phosphorylation lowers the MT stabilizing activity of these MAPs (Vandre et al., 1991, Andersen et al., 1994, Ookata et al., 1995). These MAPs may regulate cell cycle changes in MT dynamics by suppressing catastrophes and increasing rescue in interphase. Op18 is a good candidate for a protein that actively increases the frequency of MT catastrophes in mitosis. Preliminary results from Op18 depletion in extracts suggests that it may play a role in keeping non-spindle MTs depolymerized. XKCM1 could also play a role in this, however, immunolocalization reveals that the majority of this motor protein is localized to centromeric and centrosomal regions (Walczak et al, 1995). The authors of this work favor a model in which XKCM1 acts primarily to regulate dynamics of MTs attached to kinetochores. Severing factors may play a role in breaking down the long MT arrays when cells are transiting from interphase to mitosis. Alternatively they may play a role in flux. Spindles exhibit a flux of tubulin subunits towards the spindle pole even in the presence of DMSO (Sawin and Mitchison, 1994). Since MT severing proteins can sever stabilized MTs they are a likely candidate for the factor that causes subunit loss at the centrosome. The cell cycle dependent

functions and cellular localization of these MT regulators are depicted in figure 1.

REFERENCES

Andersen, S. S., Buendia, B., Dominguez, J. E., Sawyer, A., and Karsenti, E. (1994). Effect on microtubule dynamics of XMAP230, a microtubule-associated protein present in Xenopus laevis eggs and dividing cells. J Cell Biol *127*, 1289-99.

McNally, F. J., and Vale, R. D. (1993). Identification of katanin, an ATPase that severs and disassembles stable microtubules. Cell *75*, 419-29.

Ookata, K., Hisanaga, S., Bulinski, J. C., Murofushi, H., Aizawa, H., Itoh, T. J., Hotani, H., Okumura, E., Tachibana, K., and Kishimoto, T. (1995). Cyclin B interaction with microtubule-associated protein 4 (MAP4) targets p34cdc2 kinase to microtubules and is a potential regulator of M-phase microtubule dynamics. J Cell Biol *128*, 849-62.

Sawin, K. E., and Mitchison, T. J. (1994). Microtubule flux in mitosis is independent of chromosomes, centrosomes, and antiparallel microtubules. Molec. Biol. of the Cell *5*, 217-26.

Shiina, N., Gotoh, Y., Kubomura, N., Iwamatsu, A., and Nishida, E. (1994). Microtubule severing by elongation factor 1 alpha. Science *266*, 282-5.

Shiina, N., Gotoh, Y., and Nishida, E. (1992). A novel homo-oligomeric protein responsible for an MPF-dependent microtubule-severing activity. Embo J *11*, 4723-31.

Vandecandelaere, A., Martin, S. R., and Bayley, P. M. (1995). Regulation of microtubule dynamic instability by tubulin-GDP. Biochemistry *34*, 1332-43.

Vandre, D. D., Centonze, V. E., Peloquin, J., Tombes, R. M., and Borisy, G. G. (1991). Proteins of the mammalian mitotic spindle: phosphorylation/ dephosphorylation of MAP-4 during mitosis. J Cell Sci *98*, 577-88.

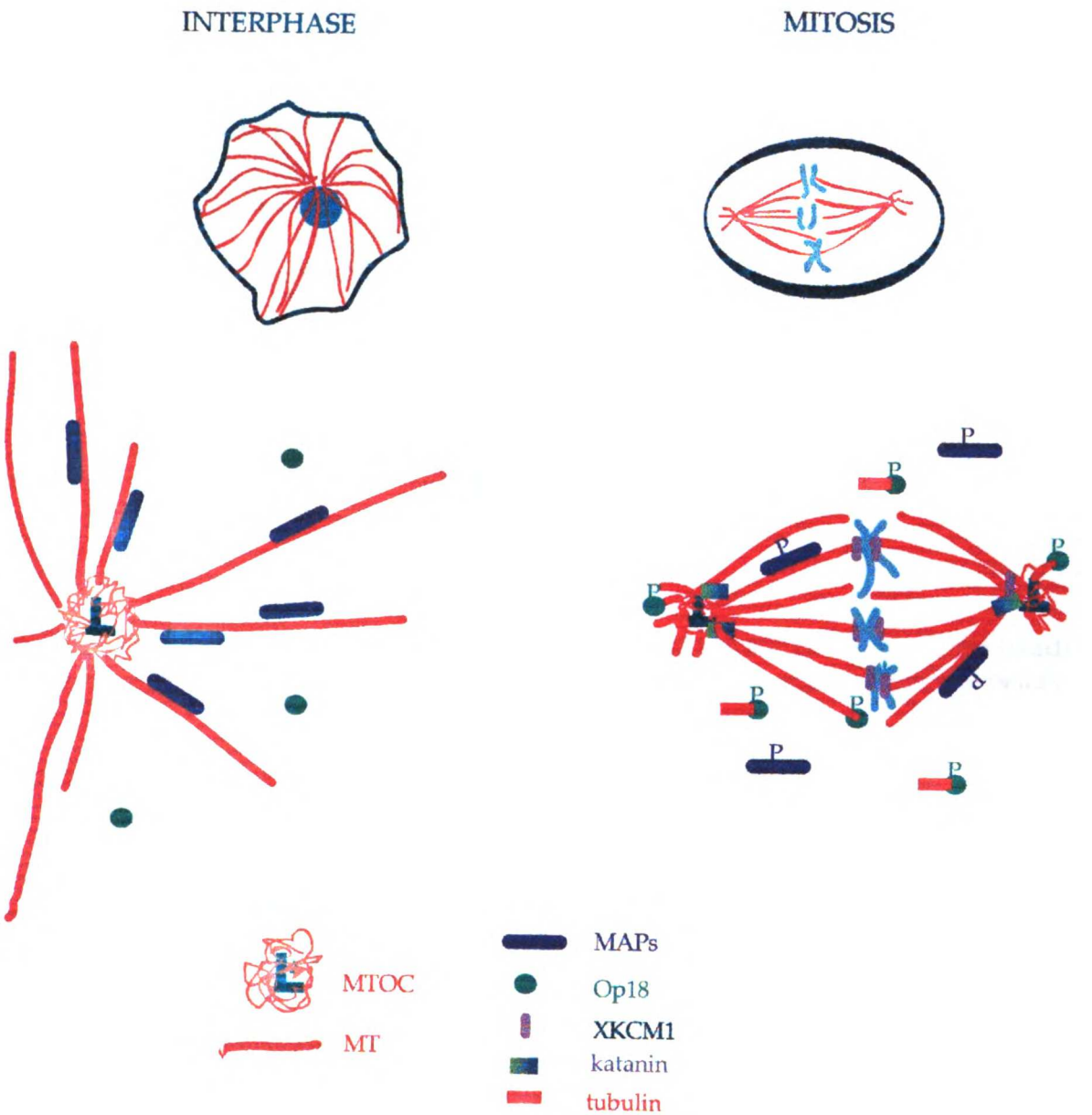
INTERPHASE
MITOSIS
P
MTOC
MT
MAPs
Op18
XKCM1
katanin
tubulin

Appendix 1 MT/MAP Depleted Extracts

Dilute crude Xenopus extract with an equal volume of cold BRB80 + Protease Inhibitors (LPC 20μg/ml) and 0.2% BME.

spin at 100K rpm 30' in TLA 100.3 or 100.4 rotor in tabletop ultra

to the sup add taxol to 20μM and GTP to 1mM

incubate 20' on ice

spin 15' 100K in TLA 100.3 15^0C

to sup add taxol to 5μM

incubate room temp 10'

spin 15' 100K in TLA100.3

tranfer sup to a tube containing 1/5 volume of packed SM2 bio-beads(BioRad) equilibrated with BRB80.

rotate in the cold for 1 hr

pellet the beads and transfer the sup to a new tube with 1/5 volume bio-beads (a syringe with a 27g needle works well for removing the sup and not the beads)

rotate in the cold 1 hr

This protocol gave a final depleted sup with 0.025 mg/ml tubulin, starting with a high speed sup with 1 mg/ml tubulin, as estimated from a Western blot. XMAP was detected only in the MT pellets, not in the taxol sups. No taxol was left in the final sup as assayed by looking for the presence of cold stable MTs upon addition of tubulin.

Appendix 2 Microtubule GTPase Assay

The following conditions were used for asays designed to identify factors that increase the GTPase rate at the plus ends of microtubules.

-Mix on ice to a final volume of 145.5 µl to give the following final concntrations of tubulin (12 mg/ml), rhodamine tubulin (0.33 mg/ml), GMPCPP (1mM) in assay buffer (AB) or BRB80.

-Incubate on ice for 10'.

-Incubate at 37°C for 10'.

-Add taxol to 100 µM.

-Layer onto warm 2.5 ml cushion of 60% glycerol, 0.1%2-ME, 2µM taxol in a TLA 100.4 tube.

-Pellet 20' at 80K rpm in the TLA 100.4 at 35°C.

-Wash cushion 3 times, wash pellet once with warm buffer

-Resuspend in 160 µl of AB with 100µM taxol at room temperature

-Dilute 20 µCi of α^{32}P GTP into a final volume of 47 µl in AB.

-Add 10 µl of MTs to each TLA100 tube.

GTPase Assay

-At t=0, add 3µl of hot GTP mix.

-At t=3', add 50 µl of the fration to be assayed (room temperature).

-At t=15', spin in TLA100 2' at 25°C, 100K rpm.

-At t=21' add the sup to 100 µl of STOP (8M urea, 20 mMEDTA, Tris pH 8.5), wash pellet with 100µl room temperature AB.

-At t=24' add 20 µl STOP to pellet, pipette to mix.

TLC

-Spot 1 µl each of 10 mM GTP and GDP onto spots 1.2 to 1.5 cm apart (mark with pencil) on a PEI (UV) TLC plate. On top of these spots pipette either 2 µl of the pellet or 3 µl of the supernatent.

-Run in 1.4 M LiCl until the solvent is nearly to the top. Visualize the spots with UV (short wavelength), dry the plate and quantitate the hydrolysis in the phospho-imager (20 to 30').

This assay was not very useful useful for the identification of novel regulators of MT dynamics because there were too many false positives. It may be of use in characterizing factors that have been shown to regulate MT asembly by other criteria.

UC San Francisco LIBRARY
UNIVERSITY OF CALIFORNIA

For reference

Not to be taken from the room.

6462553

3 1378 00646 2553

UC San Francisco LIBRARY

UNIVERSITY OF CALIFORNIA